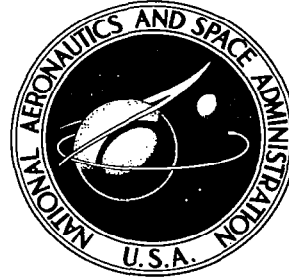


NASA  
CR  
2258  
c.1



# NASA CONTRACTOR REPORT

NASA CR-2258

NASA CR-2258



LOAN COPY: RETURN TO  
AFWL TECHNICAL LIBRARY  
KIRTLAND AFB, N. M.

## DEVELOPMENT OF A NONLINEAR UNSTEADY TRANSONIC FLOW THEORY

*by Stephen S. Stahara and John R. Spreiter*

*Prepared by*  
NIELSEN ENGINEERING & RESEARCH, INC.  
Mountain View, Calif. 94040  
*for Langley Research Center*

NATIONAL AERONAUTICS AND SPACE ADMINISTRATION • WASHINGTON, D. C. • JUNE 1973



0061216

1. Report No. NASA CR-2258		2. Government Accession No.		3. Recipient's Catalog No.	
4. Title and Subtitle DEVELOPMENT OF A NONLINEAR UNSTEADY TRANSONIC FLOW THEORY				5. Report Date June 1973	
				6. Performing Organization Code	
7. Author(s) Stephen S. Stahara and John R. Spreiter*				8. Performing Organization Report No. NEAR TR 46	
9. Performing Organization Name and Address Nielsen Engineering and Research, Inc. Mountain View, California				10. Work Unit No. 742-73-01-05-23	
				11. Contract or Grant No. NAS1-11567	
12. Sponsoring Agency Name and Address National Aeronautics and Space Administration Washington, D.C. 20546				13. Type of Report and Period Covered Contractor Report	
				14. Sponsoring Agency Code	
15. Supplementary Notes *Stanford University, Stanford, California					
16. Abstract <p>A preliminary investigation was conducted to develop the basis of a nonlinear, unsteady, small-disturbance theory capable of predicting inviscid transonic flows about aerodynamic configurations undergoing both rigid body and elastic oscillations. The theory is based on the concept of dividing the flow into steady and unsteady components and then solving, by the method of local linearization, the coupled differential equation for the unsteady surface pressure distribution.</p> <p>The appropriate equations, valid at all frequencies, have been derived for two-dimensional flows at <math>M_\infty \approx 1</math>, and numerical results obtained for two classes of airfoils and two types of oscillatory motions. The results indicate that the theory smoothly and correctly converges to nonlinear quasi-steady theory as the reduced frequency of oscillation <math>k \rightarrow 0</math> and to linear acoustic theory as <math>k</math> becomes large (<math>k \geq 2</math>). Moreover, at low frequencies (<math>k \approx 0.1</math>) the theory shows quantitatively the large nonlinear thickness effects induced on the unsteady flow by the steady motion and the complete inadequacy of linear theory in this frequency regime.</p>					
17. Key Words (Suggested by Author(s)) Flutter Unsteady aerodynamics Transonic theory				18. Distribution Statement Unclassified - Unlimited	
19. Security Classif. (of this report) Unclassified		20. Security Classif. (of this page) Unclassified		21. No. of Pages 46	22. Price* \$3.00



TABLE OF CONTENTS

	<u>Page No.</u>
SUMMARY . . . . .	1
INTRODUCTION . . . . .	1
LIST OF SYMBOLS . . . . .	2
ANALYSIS . . . . .	5
Partial Differential Equations . . . . .	5
General Oscillatory Motions . . . . .	7
Similarity Equations for Two-Dimensional Flows . . . . .	9
Local Linearization Method . . . . .	12
Edge Correction for Subsonic Potential . . . . .	17
Similarity Equations for Axisymmetric Flows . . . . .	18
RESULTS AND DISCUSSION . . . . .	21
CONCLUDING REMARKS . . . . .	24
REFERENCES . . . . .	26
FIGURES 1 THROUGH 13 . . . . .	28

## DEVELOPMENT OF A NONLINEAR UNSTEADY

### TRANSONIC FLOW THEORY

By Stephen S. Stahara and John R. Spreiter\*  
Nielsen Engineering & Research, Inc.

#### SUMMARY

A preliminary investigation was conducted to develop the basis of a nonlinear, unsteady, small-disturbance theory capable of predicting inviscid transonic flows about aerodynamic configurations undergoing both rigid body and elastic oscillations. The theory is based on the concept of dividing the flow into steady and unsteady components and then solving, by the method of local linearization, the coupled differential equation for the unsteady surface pressure distribution.

The appropriate equations, valid at all frequencies, have been derived for two-dimensional flows at  $M_\infty \approx 1$ , and numerical results obtained for two classes of airfoils and two types of oscillatory motions. The results indicate that the theory smoothly and correctly converges to nonlinear quasi-steady theory as the reduced frequency of oscillation based on chord  $\bar{k} \rightarrow 0$  and to linear acoustic theory as  $\bar{k}$  becomes large ( $\bar{k} \gtrsim 2$ ). Moreover, at low frequencies ( $\bar{k} \approx 0.1$ ) the theory shows quantitatively the large nonlinear thickness effects induced on the unsteady flow by the steady motion and the complete inadequacy of linear theory in this frequency regime.

#### INTRODUCTION

The basic reason for developing an accurate unsteady transonic flow theory lies in the need to predict aerodynamic flutter and its associated dynamic instabilities, which are more likely to occur in the transonic regime than in any other. In view of emerging technological needs, however, such as those associated with the design of a transonic transport, the present state of unsteady transonic aerodynamics is clearly inadequate.

---

\*Professor, Departments of Applied Mechanics and Aeronautics and Astronautics, Stanford University, Stanford, California. (Consultant at Nielsen Engineering & Research, Inc.).

While some work has been done (see refs. 1-4), such technically important problems as one-degree-of-freedom control surface flutter (control surface buzz) and the determination of stability derivatives at low reduced frequencies, to say nothing of the more general problem of predicting pressures on arbitrary oscillating surfaces at transonic speeds, remain essentially unsolved at the present time. Unless the frequency of oscillation is sufficiently high or the configuration of a special nature, agreement of existing theoretical results and data is not satisfactory (ref. 3). The reason for these discrepancies stems from the linearization of the governing differential equations, which are fundamentally nonlinear in this speed regime. Consequently, it is clear that an adequate analysis of unsteady transonic flows must include at least some of the nonlinear effects present and one of the goals of this investigation is to identify and include the most important of these effects.

Perhaps the primary reason for the relatively slow development of unsteady transonic aerodynamics is that, until recently, there existed a notable paucity of techniques for accurately predicting the steady transonic flow about realistic aerodynamic shapes. Current research, however, has changed that situation so that the accurate theoretical treatment of realistic two- and three-dimensional steady transonic flows (refs. 5-10) is now possible. This is of major importance to the present technique which makes use of the nonlinear steady solution in determining the unsteady flow.

Although the ultimate goal of this investigation is to evolve predictive methods for calculating unsteady pressures, forces, and moments acting on general aerodynamic configurations throughout the transonic regime, the purpose of this preliminary study is to develop the basis of a nonlinear unsteady theory capable of accurately predicting transonic flows about airfoils undergoing both rigid-body and elastic oscillations.

#### LIST OF SYMBOLS

$A_1$  equal to  $\lambda_2/2\lambda_1$   
 $A_2$  equal to  $(\lambda_2/2\lambda_1) \cdot \sqrt{1 - 4\lambda_1\lambda_3/\lambda_2^2}$

$c$	reference length: for two-dimensional flows, equal to chord length; for axisymmetric flows, equal to body length
$C_p$	total pressure coefficient, equations (26) and (71)
$C_{p_1}$	steady-state pressure coefficient, equation (25)
$\tilde{C}_p$	unsteady pressure coefficient, equation (25)
$\bar{C}_p$	similarity form of steady pressure coefficient, equations (27) and (72)
$\hat{C}_p$	similarity form of unsteady pressure coefficient, equations (28) and (73)
$f$	equal to $d\tilde{Z}(x)/dx + i\bar{k}\tilde{Z}(x)$
$F$	function describing body surface, equation (11)
$g$	equal to $\bar{R}(x) [d\tilde{R}(x)/dx + i\bar{k}\tilde{R}(x)]$
$I_0$	zero-order modified Bessel function of first kind
$\bar{k}$	reduced oscillatory frequency based on chord, $\omega c/U_\infty$
$K_0$	zero-order modified Bessel function of second kind
$K_1$	similarity parameter, equal to $M_\infty^2 - 1 / [M_\infty^2 (\gamma + 1)]^{2/3}$
$K_2$	similarity parameter, equal to $2\bar{k}/\varepsilon(\gamma + 1)$ , equations (24) and (70)
$M_\infty$	free stream Mach number
$R$	dimensionless total body radius, normalized by $c$ ; equation (60)
$\bar{R}$	dimensionless affine function describing steady-state body radius, equation (60)
$\tilde{R}$	dimensionless affine function describing amplitude of unsteady radial perturbation, equation (60)
$t$	nondimensional time, normalized by $c/U_\infty$
$U_\infty$	free stream-velocity

$(x, y, z)$  nondimensional, body-fixed Cartesian coordinate system with  $x$  axis directed rearward and aligned with longitudinal axis of body,  $y$  axis directed to the right facing forward, and  $z$  axis directed vertically upward; coordinates normalized by  $c$

$x^*$  location of steady-state sonic point, normalized by  $c$

$Z$  dimensionless total wing or airfoil ordinates, normalized by  $c$ ; equation (9)

$Z_1$  dimensionless steady-state airfoil ordinates, normalized by  $c$ ; equation (79)

$\bar{Z}$  dimensionless affine function describing steady-state wing or airfoil ordinates, equation (9)

$\tilde{Z}$  dimensionless affine function describing amplitude of unsteady wing or airfoil ordinate perturbation, equation (9)

$\gamma$  ratio of specific heats

$\delta$  dimensionless amplitude of unsteady oscillation, normalized by  $c$

$\epsilon$  expansion parameter for steady flow, equations (16) and (63)

$\epsilon_1$  expansion parameter for unsteady flow, equations (17) and (64)

$\zeta$  normalized similarity form of  $z$  ordinate, equation (18)

$\lambda_1$  equal to  $\bar{\Phi}_x + K_1$

$\lambda_2$  equal to  $\bar{\Phi}_{xx} + iK_2$

$\lambda_3$  equal to  $-\bar{k}K_2/2$

$\xi, \xi_1$  dummy variables

$\rho$  normalized similarity form of radial ordinate, equation (65)

$\tau$  airfoil, wing, or body thickness ratio

$\phi$  dimensionless total perturbation velocity potential, equations (6) and (59)

$\phi_1$  dimensionless steady-state perturbation velocity potential, equations (6) and (59)

$\tilde{\phi}$  amplitude of dimensionless unsteady perturbation velocity potential, equations (6) and (59)



$\bar{\phi}$	similarity form of dimensionless steady-state perturbation velocity potential, equations (14) and (61)
$\tilde{\phi}$	similarity form of dimensionless unsteady perturbation velocity potential, equations (15) and (62)
$\Delta\tilde{\phi}$	edge-correction potential to $\tilde{\phi}$ for subsonic flow, equation (58)
$\omega$	oscillatory frequency, rad/sec

## ANALYSIS

### Partial Differential Equations

The concept that a major body of steady transonic flow problems can be predicted accurately within the framework of inviscid, small-disturbance theory without recourse to numerical solutions of the full nonlinear equations has been established (refs. 11 and 12) for some time. There is good reason to believe that this premise also holds for the unsteady case, particularly for small-amplitude flutter and stability calculations. For unsteady motions, small-disturbance transonic theory yields the following differential equation for the dimensionless perturbation velocity potential  $\phi$  (ref. 3)

$$(1 - M_{\infty}^2)\phi_{xx} + \phi_{yy} + \phi_{zz} = M_{\infty}^2(\gamma + 1)\phi_x\phi_{xx} + M_{\infty}^2\phi_{tt} + 2M_{\infty}^2\phi_{xt} \quad (1)$$

where  $M_{\infty}$  is the free-stream Mach number,  $\gamma$  is the ratio of specific heats,  $(x,y,z)$  are the spatial coordinates nondimensionalized by some reference length  $c$ , and  $t$  is the nondimensional time normalized by  $c/U_{\infty}$ .

Depending upon the nature of the unsteady motion, equation (1) can simplify into various forms. For very fast oscillations, the following linear, two-dimensional wave equation holds,

$$\phi_{yy} + \phi_{zz} = M_{\infty}^2\phi_{tt} \quad (2)$$

while for slightly slower unsteady motions, the more complicated linear equation is valid.

$$(1 - M_{\infty}^2)\phi_{xx} + \phi_{yy} + \phi_{zz} = M_{\infty}^2\phi_{tt} + 2M_{\infty}^2\phi_{xt} \quad (3)$$

For slowly unsteady motion, the following nonlinear equation applies,

$$(1 - M_\infty^2)\phi_{xx} + \phi_{yy} + \phi_{zz} = M_\infty^2(\gamma + 1)\phi_x\phi_{xx} + 2M_\infty^2\phi_{xt} \quad (4)$$

while for very slow (quasi-steady) motions, the same nonlinear equation that holds for steady flow applies.

$$(1 - M_\infty^2)\phi_{xx} + \phi_{yy} + \phi_{zz} = M_\infty^2(\gamma + 1)\phi_x\phi_{xx} \quad (5)$$

Solutions to the linear two-dimensional wave equation (eq. (2)) are straightforward and not of primary concern here. Miles (ref. 13) has treated the linear equation (3) by analytical means for supersonic flows, while Landahl (ref. 1) has applied the same equation at  $M_\infty = 1$  to certain classes of wings and low aspect ratio wing-body combinations. While many important applications remain to be worked out for this equation, it is clear from past comparisons with experimental data that some of the nonlinear features characteristic to problems in this speed regime, which have been omitted by this equation, must be included.

Very little work has been done on solving the more difficult nonlinear equation (4). In many practical flutter and stability problems, the reduced frequencies are very low and in investigations of dynamic stability, the values of aerodynamic stability derivatives as the reduced frequency  $\bar{k} \rightarrow 0$  are required. Furthermore, it can be shown by the method of matched asymptotic expansions that equation (4) provides the proper solution for a relatively wide range of low frequency unsteady motions and that the solutions of equation (4) converge uniformly as  $\bar{k} \rightarrow 0$  to the nonlinear quasi-steady results provided by equation (5). Thus, solutions to equation (4) contain information about both low frequency and quasi-steady nonlinear motions. Consequently, while in this study we will seek solutions to the more general nonlinear unsteady small-disturbance equation (1), we note that for low frequency motions the simpler nonlinear equation (4) could be legitimately used.

Finally, with regard to steady-state solutions of the nonlinear equation (5), several comments are appropriate. First, it has been adequately demonstrated (refs. 11 and 12) that solutions of this equation are capable of providing good representations of actual steady transonic flows about a wide variety of shapes. Applications to thin airfoils (refs. 14, 15, and 16) finite-span wings (ref. 17), slender bodies of revolution (refs. 15,

18, and 19), slender nonaxisymmetric bodies (ref. 8), and even certain classes of wing-body combinations (refs. 8, 9, and 10) have confirmed this. Consequently, the nonlinear effects associated with a major body of transonic flows can be adequately accounted for by inclusion of the  $\phi_x \phi_{xx}$  term in equation (5). Furthermore, at this time both exact and approximate methods for solving this equation are available as indicated above (refs: 5, 6, and 7).

### General Oscillatory Motions

Fundamental to any study of unsteady aerodynamics is the analysis of oscillatory motion. For general oscillatory motions, it is convenient to expand the solution into a steady and unsteady component. Thus, we may set

$$\phi(x,y,z,t) = \phi_1(x,y,z) + \text{R.P.} \left\{ \tilde{\phi}(x,y,z) e^{i\bar{k}t} \right\} \quad (6)$$

where  $k$  is the reduced frequency of the oscillatory motion, R.P. signifies the real part of the complex quantity,  $\phi_1$  is the steady perturbation potential, and  $\tilde{\phi}$  is the amplitude of the oscillatory potential. Inserting equation (6) into the full equation (1), the following coupled partial differential equation is obtained for  $\tilde{\phi}$ .

$$\begin{aligned} (1 - M_\infty^2) \tilde{\phi}_{xx} + \tilde{\phi}_{yy} + \tilde{\phi}_{zz} = M_\infty^2 (\gamma + 1) (\tilde{\phi}_x \tilde{\phi}_{xx} + \phi_{1x} \tilde{\phi}_{xx} + \phi_{1xx} \tilde{\phi}_x) \\ - M_\infty^2 \bar{k}^2 \tilde{\phi} + 2iM_\infty^2 \bar{k} \tilde{\phi}_x \end{aligned} \quad (7)$$

This equation has variable coefficients, is both nonlinear and of mixed elliptic-hyperbolic type and is, in general, more difficult to solve than the corresponding one for the steady component (eq. (5)). Since, in flutter and stability analysis, the stability of only small-amplitude oscillations is normally investigated, it is appropriate to assume that the oscillatory flow is a small perturbation on the nonlinear steady flow. This is logical inasmuch as oscillations or other unsteady deformations of the surfaces of an aircraft should involve only minor deviations from their steady-state positions. With this simplification, the governing equation for  $\tilde{\phi}$  becomes

$$(1 - M_\infty^2) \tilde{\phi}_{xx} + \tilde{\phi}_{yy} + \tilde{\phi}_{zz} = M_\infty^2 (\gamma + 1) (\phi_{1x} \tilde{\phi}_{xx} + \phi_{1xx} \tilde{\phi}_x) + 2iM_\infty^2 \bar{k} \tilde{\phi}_x - M_\infty^2 \bar{k}^2 \tilde{\phi} \quad (8)$$

which, although being linear remains quite formidable to solve because of the variable coefficients and mixed elliptic-hyperbolic type. It is likely, however, that solutions of this equation will provide all of the information necessary for an accurate transonic stability analysis.

With the above approach of splitting the perturbation potential, the surface boundary condition can be treated in a very general way, accounting for both rigid body and elastic oscillations. For example, for thin wings where  $Z(x,y,t)$  represents the normalized ordinates of the upper surface, we can set

$$Z(x,y,t) = \tau \bar{Z}(x,y) + \text{R.P.} \left\{ \delta \tilde{Z}(x,y) e^{i\bar{k}t} \right\} \quad (9)$$

where  $\tau$  and  $\delta$  represent, respectively, the wing thickness ratio and the normalized amplitude of the unsteady oscillation. In this representation rigid body plunging oscillations can be given by  $\tilde{Z}(x,y) = 1$ , pitching oscillations about a line at  $x = x_0$  by  $\tilde{Z}(x,y) = (x - x_0)$ , elastic longitudinal oscillations by  $\tilde{Z}(x,y) = f(y) \sin(n\pi x)$ , etc. Solutions for more general unsteady motions such as gust response, buffeting, etc., can be obtained by superposition of such oscillatory solutions.

The surface boundary condition for the oscillatory component is found from the expression

$$\frac{\partial F}{\partial t} + \text{grad}(x + \phi) \cdot \text{grad} F = 0 \quad \text{on} \quad F(x,y,z,t) = 0 \quad (10)$$

where

$$F(x,y,z,t) = z - Z(x,y,t) \quad (11)$$

with  $\phi$  given by equation (6) and  $Z(x,y,t)$  by equation (9). Thus,

$$\tilde{\phi}_z(x,y,0\pm) = \pm \delta \left[ \frac{\partial \tilde{Z}(x,y)}{\partial x} + i\bar{k} \tilde{Z}(x,y) \right] \quad (12)$$

At infinity, the unsteady velocity components must vanish in an appropriate fashion.

In transonic and supersonic flows, it is also necessary, in general, to provide appropriate relations for the discontinuous changes in velocity that occur at shock surfaces. However, in the case of sonic and near-sonic flows which are considered in this report, for large classes of thin airfoils and wings with convex contours at zero or small angles of attack, the shock waves present originate at the trailing edge. For small amplitude oscillations, they remain substantially fixed at that location and do not require further attention. However, we note that in general even for these classes of shapes, at Mach numbers in the lower transonic regime when shock waves appear on the upper and/or lower surface and at Mach numbers in the upper transonic regime when bow shocks appear, these shock relations must be properly accounted for.

Finally, the pressure coefficient for the thin wing case is given by

$$C_p = -2 \left[ \phi_{1,x} + \text{R.P.} \left\{ \tilde{\phi}_x + i\bar{k}\tilde{\phi} \right\} e^{i\bar{k}t} \right] \quad (13)$$

while for slender bodies additional terms, as usual, appear (see Similarity Equations for Axisymmetric Flows).

#### Similarity Equations for Two-Dimensional Flows

By using the method of matched asymptotic expansions, it can be shown that for two-dimensional flow the potentials  $(\phi_1, \tilde{\phi})$  can be expressed in the similarity form

$$\phi_1(x, z) = \varepsilon \bar{\Phi}(x, \zeta) + O(\varepsilon^2) \quad (14)$$

$$\tilde{\phi}(x, z) = \varepsilon_1 \tilde{\Phi}(x, \zeta) + O(\varepsilon_1^2) \quad (15)$$

where

$$\varepsilon = \left[ \frac{\tau^2}{M_\infty^2 (\gamma + 1)} \right]^{1/3} \quad (16)$$

$$\varepsilon_1 = \frac{\delta}{\left[ \tau M_\infty^2 (\gamma + 1) \right]^{1/3}} \quad (17)$$

$$\zeta = \left[ M_\infty^2 (\gamma + 1) \tau \right]^{1/3} z \quad (18)$$

and the similarity potentials  $(\bar{\Phi}, \tilde{\Phi})$  satisfy the following differential equations and boundary conditions

$$-\left[ K_1 + \bar{\Phi}_x \right] \bar{\Phi}_{xx} + \bar{\Phi}_{\zeta\zeta} = 0 \quad (19)$$

$$\bar{\Phi}_\zeta(x, 0\pm) = \pm \frac{d\bar{Z}(x)}{dx} \quad (20)$$

and

$$-\left[ K_1 + \bar{\Phi}_x \right] \tilde{\Phi}_{xx} + \tilde{\Phi}_{\zeta\zeta} = \left[ \bar{\Phi}_{xx} + iK_2 \right] \tilde{\Phi}_x - \frac{\bar{k}}{2} K_2 \tilde{\Phi} \quad (21)$$

$$\tilde{\Phi}_\zeta(x, 0\pm) = \pm \left[ \frac{d\tilde{Z}(x)}{dx} + i\bar{k}\tilde{Z}(x) \right] \quad (22)$$

where

$$K_1 = \frac{M_\infty^2 - 1}{\left[ M_\infty^2 \tau (\gamma + 1) \right]^{2/3}} \quad (23)$$

$$K_2 = \frac{2}{\gamma + 1} \frac{\bar{k}}{\varepsilon} = 2\bar{k} \left[ \frac{M_\infty}{\tau(\gamma + 1)} \right]^{2/3} \quad (24)$$

The physical pressure coefficient  $C_p$  can be represented by

$$C_p = C_{p_1} + \text{R.P.} \left\{ \tilde{C}_p e^{i\bar{k}t} \right\} \quad (25)$$

with  $\tilde{C}_p$  defined by equation (13), or in similarity form by

$$C_p = \varepsilon \bar{C}_p + \varepsilon_1 \text{R.P.} \left\{ \hat{C}_p e^{i\bar{k}t} \right\} \quad (26)$$

where  $\bar{C}_p$  and  $\hat{C}_p$  are the similarity forms of the steady and unsteady pressure coefficients and are given by

$$\bar{C}_p = -2 \bar{\phi}_x \quad (27)$$

$$\hat{C}_p = -2 \left\{ \tilde{\phi}_x + i\bar{k}\tilde{\phi} \right\} \quad (28)$$

Thus, the differential equation and boundary condition for the unsteady component can be expressed in the compact form

$$\lambda_1 \tilde{\phi}_{xx} + \lambda_2 \tilde{\phi}_x + \lambda_3 \tilde{\phi} = \tilde{\phi}_{\zeta\zeta} \quad (29)$$

$$\tilde{\phi}_\zeta(x, 0\pm) = \pm f(x) \quad (30)$$

where

$$\lambda_1 \equiv K_1 + \bar{\phi}_x \quad (31)$$

$$\lambda_2 \equiv \dot{\bar{\phi}}_{xx} + iK_2 \quad (32)$$

$$\lambda_3 \equiv -\frac{\bar{K}}{2} K_2 \quad (33)$$

$$f(x) \equiv \frac{d\tilde{Z}(x)}{dx} + i\bar{k}\tilde{Z}(x) \quad (34)$$

so that, depending upon the value of  $\lambda_1$ , the following set of equations must be solved:

(1) Sonic Equation ( $x = x^*$ ,  $\lambda_1 = 0$ )

$$\lambda_2 \tilde{\phi}_x + \lambda_3 \tilde{\phi} = \tilde{\phi}_{\zeta\zeta} \quad (\text{R.P. } \{\lambda_2\} > 0) \quad (35)$$

(2) Supersonic Equation ( $x > x^*$ ,  $\lambda_1 > 0$ )

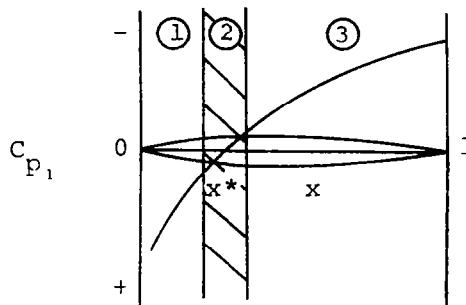
$$\lambda_1 \tilde{\phi}_{xx} + \lambda_2 \tilde{\phi}_x + \lambda_3 \tilde{\phi} = \tilde{\phi}_{\zeta\zeta} \quad (36)$$

(3) Subsonic Equation ( $x < x^*$ ,  $\lambda_1 < 0$ )

$$(-\lambda_1) \tilde{\phi}_{xx} - \lambda_2 \tilde{\phi}_x - \lambda_3 \tilde{\phi} + \tilde{\phi}_{\zeta\zeta} = 0 \quad (37)$$

where  $x^*$  denotes the location of the steady flow sonic point, i.e., where  $\lambda_1 = 0$ .

The occurrence of the three fundamentally different equations for  $\tilde{\phi}$  is necessary and is a result of the unsteady flow disturbances riding on the basic characteristics of the steady flow which contains subsonic ( $\lambda_1 < 0$ ), sonic ( $\lambda_1 = 0$ ), and supersonic ( $\lambda_1 > 0$ ) regions. The regions in which the various solutions will apply can be seen more clearly in the figure below, which represents schematically the typical steady surface pressure distribution on a thin, convex airfoil at  $M_\infty = 1$ .



The solution for the sonic region (2) must merge continuously with that for the subsonic region (1) ahead of it and the supersonic region (3) behind it.

With regard to the  $\lambda_3 \tilde{\phi}$  term which appears in the preceding equations, if we were to restrict the analysis to slowly unsteady nonlinear motions, then this term, which results from the  $M_\infty^2 \phi_{tt}$  term in equation (1), could be legitimately omitted (cf. eqs. (1) and (4)). However, it appears that no undue complications arise from retaining this term. Consequently, the analysis and theory presented in this report are applicable, without restriction, to all frequencies.

#### Local Linearization Method

The local linearization method, originated by Spreiter and Alksne (refs. 14, 17, and 18), was developed as an approximate method for solving the nonlinear transonic steady flow equation (5), although the basic ideas of the technique are apparently applicable to a large number of both linear and nonlinear problems. It has been applied successfully in the past to transonic flows past a wide variety of thin airfoils (refs. 14, 15, and 16),

slender bodies of revolution (refs. 15, 18, and 19) and wings of finite span (ref. 17), and more recently to even more complex shapes, including nonaxisymmetric bodies and wing-body combinations (refs. 8, 9, and 10). With regard to the present problem, the procedure for determining the local linearization solution for the unsteady component  $\tilde{\phi}$  is to replace temporarily the variable coefficients ( $\lambda_1, \lambda_2$ ) by constants, solve the simplified equations (35), (36), and (37) for  $\tilde{\phi}(x, \zeta)$ , calculate the unsteady surface acceleration  $d^2\tilde{\phi}(x, 0)/dx^2$ , then replace the constants ( $\lambda_1, \lambda_2$ ) by the functions they originally represented, and finally integrate the resultant second-order ordinary differential equation to obtain both  $\tilde{\phi}_x(x, 0)$  and  $\tilde{\phi}(x, 0)$  as are required (see eq. (13)) to determine the unsteady surface pressure.

Solutions of equations (35), (36), and (37) with ( $\lambda_1, \lambda_2$ ) as constants have been determined and are given for the sonic case ( $\lambda_1 \approx 0$ ) by

$$(\tilde{\phi}(x, \zeta))_{\text{sonic}} = \frac{-1}{\sqrt{\pi\lambda_2}} \int_0^x \frac{f(\xi)e^{-\frac{\lambda_3}{\lambda_2}(x-\xi) - \frac{\lambda_2\zeta^2}{4(x-\xi)}}}{\sqrt{x-\xi}} d\xi \quad (38)$$

for the supersonic case ( $\lambda_1 > 0$ ) by

$$(\tilde{\phi}(x, \zeta))_{\text{supersonic}} = \frac{-1}{\sqrt{\lambda_1}} \int_0^x f(\xi)e^{-\sqrt{\lambda_1}\zeta - A_1(x-\xi)} I_0 \left[ A_2 \sqrt{(x-\xi)^2 - \lambda_1\zeta^2} \right] d\xi \quad (39)$$

and for the subsonic case ( $\lambda_1 < 0$ ) by

$$(\tilde{\phi}(x, \zeta))_{\text{subsonic}} = \frac{-1}{\pi\sqrt{-\lambda_1}} \int_0^1 f(\xi)e^{-A_1(x-\xi)} K_0 \left[ -A_2 \sqrt{(x-\xi)^2 + (-\lambda_1)\zeta^2} \right] d\xi \quad (40)$$

where  $A_1$  and  $A_2$  are defined as

$$A_1 = \frac{\lambda_2}{2\lambda_1} \quad (41)$$

$$A_2 = \frac{\lambda_2}{2\lambda_1} \sqrt{1 - \frac{4\lambda_1\lambda_3}{\lambda_2^2}} \quad (42)$$

and where  $I_0$  and  $K_0$  are zero-order modified Bessel functions of the first and second kind, respectively. As  $x \rightarrow x^*$  (i.e., as  $\lambda_1 \rightarrow 0$ ), it can be shown that the supersonic and subsonic solutions (and their derivatives) given by equations (39) and (40) uniformly converge to the sonic result given by equation (38) as they must.

Application of the local linearization method, together with some manipulation to obtain forms convenient for numerical integration, provides the following second-order ordinary differential equations for the unsteady surface acceleration  $d^2\tilde{\phi}(x,0)/dx^2$ .

$$\left(\frac{d^2\tilde{\phi}(x,0)}{dx^2}\right)_{\text{sonic}} = \frac{-1}{\sqrt{\pi\lambda_2}} \left[ \frac{-f(0)e^{-\frac{\lambda_3}{\lambda_2}x}}{\sqrt{x}} \left\{ \frac{1}{2x} + \frac{\lambda_3}{\lambda_2} \right\} + \frac{f'(0)e^{-\frac{\lambda_3}{\lambda_2}x}}{\sqrt{x}} \right. \\ \left. + 2f''(x) \int_0^x e^{-\frac{\lambda_3}{\lambda_2}\xi^2} d\xi - \int_0^x \frac{\{f''(x) - f''(\xi)\} e^{-\frac{\lambda_3}{\lambda_2}(x-\xi)}}{\sqrt{x-\xi}} d\xi \right] \quad (43)$$

$$\left(\frac{d^2\tilde{\phi}(x,0)}{dx^2}\right)_{\text{super sonic}} = \frac{-1}{\sqrt{\lambda_1}} \left[ f(0)e^{-A_1x} \cdot A_1 \cdot \left\{ -I_0[A_2x] + \frac{A_2}{A_1} \cdot I_1[A_2x] \right\} \right. \\ \left. + f'(0)e^{-A_1x} \cdot I_0[A_2x] + \int_0^x f''(\xi)e^{-A_1(x-\xi)} \cdot I_0[A_2(x-\xi)] d\xi \right] \quad (44)$$

$$\left(\frac{d^2\tilde{\phi}(x,0)}{dx^2}\right)_{\text{sub sonic}} = \frac{-1}{\pi\sqrt{-\lambda_1}} \left[ f(0)e^{-A_1x} \cdot (-A_1) \cdot \left\{ K_0[-A_2x] - \frac{A_2}{A_1} K_1[-A_2x] \right\} \right. \\ \left. - f(1)e^{A_1(1-x)} \cdot (-A_1) \cdot \left\{ K_0[-A_2(1-x)] + \frac{A_2}{A_1} K_1[-A_2(1-x)] \right\} \right. \\ \left. + f'(0)e^{-A_1x} \cdot K_0[-A_2x] - f'(1)e^{A_1(1-x)} \cdot K_0[-A_2(1-x)] \right]$$

(Continued on next page)

$$\begin{aligned}
& + \int_0^x \left\{ f''(\xi) - f''(x) \right\} e^{-A_1(x-\xi)} \cdot K_0 \left[ -A_2(x-\xi) \right] d\xi \\
& + \int_x^1 \left\{ f''(\xi) - f''(x) \right\} e^{A_1(\xi-x)} \cdot K_0 \left[ -A_2(\xi-x) \right] d\xi \\
& + f''(x) \left\{ \int_0^x e^{-A_1(x-\xi)} \cdot \left\{ K_0 \left[ -A_2(x-\xi) \right] \right. \right. \\
& + \ln \left[ -A_2 \frac{(x-\xi)}{2} \right] \left. \right\} d\xi + \int_x^1 e^{A_1(\xi-x)} \cdot \left\{ K_0 \left[ -A_2(\xi-x) \right] \right. \\
& + \ln \left[ -A_2 \frac{(\xi-x)}{2} \right] \left. \right\} d\xi - \int_0^x \left\{ e^{-A_1(x-\xi)} - 1 \right\} \times \\
& \ln \left[ -A_2 \frac{(x-\xi)}{2} \right] d\xi - \int_x^1 \left\{ e^{A_1(\xi-x)} - 1 \right\} \times \\
& \ln \left[ -A_2 \frac{(\xi-x)}{2} \right] d\xi - x \left\{ \ln \left[ -A_2 \frac{x}{2} \right] - 1 \right\} \\
& - (1-x) \left\{ \ln \left[ -A_2 \frac{(1-x)}{2} \right] - 1 \right\} \left. \right\} \quad (45)
\end{aligned}$$

where now  $(\lambda_1, \lambda_2)$  and, consequently,  $(A_1, A_2)$  are functions of  $x$  only, i.e.

$$\lambda_1 = \bar{\Phi}_x(x, 0) + K_1 \quad (46)$$

$$\lambda_2 = \bar{\Phi}_{xx}(x, 0) + iK_2 \quad (47)$$

In order to integrate equations (43), (44), and (45), two boundary conditions are required. These are provided, in direct analogy to the local linearization solutions for the steady case, by requiring that at the steady-state sonic point  $x^*$

$$\tilde{\Phi}(x^*, 0) = (\tilde{\Phi}(x^*, 0))_{\text{sonic}} = \frac{-1}{\sqrt{\pi\lambda_2^*}} \int_0^{x^*} \frac{f(\xi) e^{-\frac{\lambda_3}{\lambda_2^*}(x^*-\xi)}}{\sqrt{x^*-\xi}} d\xi \quad (48)$$

$$\begin{aligned} \frac{d\tilde{\Phi}(x^*, 0)}{dx} = \left( \frac{d\tilde{\Phi}(x^*, 0)}{dx} \right)_{\text{sonic}} &= \frac{-1}{\sqrt{\pi\lambda_2^*}} \left[ \frac{f(0) e^{-\frac{\lambda_3}{\lambda_2^*} x^*}}{\sqrt{x^*}} \right. \\ &\quad \left. + \int_0^{x^*} \frac{f'(\xi) e^{-\frac{\lambda_3}{\lambda_2^*}(x^*-\xi)}}{\sqrt{x^*-\xi}} d\xi \right] \end{aligned} \quad (49)$$

where  $\lambda_2^* = \lambda_2(x^*) = \bar{\Phi}_{xx}(x^*, 0) + iK_2$ .

For numerical evaluation, more convenient forms of equations (48) and (49) are

$$\tilde{\Phi}(x^*, 0) = \frac{-1}{\sqrt{\pi\lambda_2^*}} \left[ 2f(x^*) \int_0^{\sqrt{x^*}} e^{-\frac{\lambda_3}{\lambda_2^*} \xi^2} d\xi - \int_0^{x^*} \frac{[f(x^*) - f(\xi)] e^{-\frac{\lambda_3}{\lambda_2^*}(x^*-\xi)}}{\sqrt{x^*-\xi}} d\xi \right] \quad (50)$$

$$\begin{aligned} \frac{d\tilde{\Phi}(x^*, 0)}{dx} &= \frac{-1}{\sqrt{\pi\lambda_2^*}} \left[ \frac{f(0) e^{-\frac{\lambda_3}{\lambda_2^*} x^*}}{\sqrt{x^*}} + 2f'(x^*) \int_0^{\sqrt{x^*}} e^{-\frac{\lambda_3}{\lambda_2^*} \xi^2} d\xi \right. \\ &\quad \left. - \int_0^{x^*} \frac{[f'(x^*) - f'(\xi)] e^{-\frac{\lambda_3}{\lambda_2^*}(x^*-\xi)}}{\sqrt{x^*-\xi}} d\xi \right] \end{aligned} \quad (51)$$

Although in their general form, equations (43), (44), and (45) appear formidable, for certain oscillatory motions, they simplify considerably. For example, for plunging oscillations where  $\tilde{Z}(x) = 1$  so that  $f(x) = i\bar{k}$ , we have

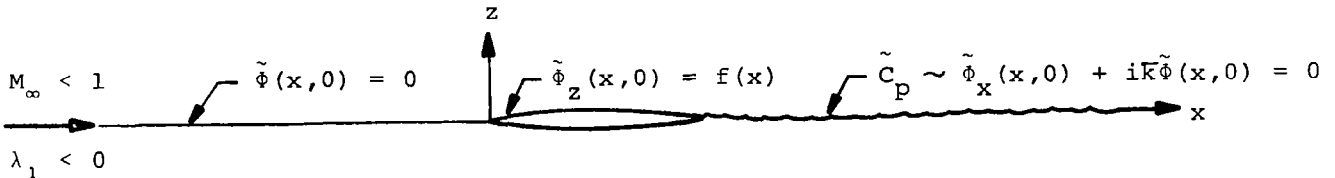
$$\left(\frac{d^2 \tilde{\Phi}(x,0)}{dx^2}\right)_{\text{sonic}} = \frac{i\bar{k}}{\sqrt{\pi\lambda_2}} e^{-\frac{\lambda_3}{\lambda_2} x} \left\{ \frac{1}{2x} + \frac{\lambda_3}{\lambda_2} \right\} \quad (52)$$

$$\left(\frac{d^2 \tilde{\Phi}(x,0)}{dx^2}\right)_{\text{super sonic}} = \frac{i\bar{k}}{\sqrt{\lambda_1}} A_1 e^{-A_1 x} \cdot \left\{ I_0 [A_2 x] - \frac{A_2}{A_1} I_1 [A_2 x] \right\} \quad (53)$$

$$\left(\frac{d^2 \tilde{\Phi}(x,0)}{dx^2}\right)_{\text{sub sonic}} = \frac{i\bar{k}}{\pi \sqrt{(-\lambda_1)}} A_1 \left[ e^{-A_1 x} \cdot \left\{ K_0 [-A_2 x] - \frac{A_2}{A_1} K_1 [-A_2 x] \right\} - e^{A_1(1-x)} \cdot \left\{ K_0 [-A_2(1-x)] + \frac{A_2}{A_1} K_1 [-A_2(1-x)] \right\} \right] \quad (54)$$

#### Edge Correction for Subsonic Potential

Because of the absence of upstream influence, the sonic and supersonic solutions given above are complete, and no further boundary conditions for the wake or for points ahead of the airfoil are required. For the subsonic solution, however, these additional conditions must be taken into account. For purely subsonic ( $\lambda_1 < 0$  everywhere) unsteady lifting flows, these requirements on  $\tilde{\Phi}$  are shown in the figure below



where the condition that  $\tilde{\Phi}(x,0) = 0$  ahead of the airfoil insures the physical requirement that no discontinuity occurs in  $\tilde{\Phi}$  when crossing the  $z = 0$  line, and the condition that  $\tilde{\Phi}_x(x,0) + i\bar{k}\tilde{\Phi}(x,0) = 0$  in the wake insures the continuity of pressure along that line. For a supersonic trailing edge, which is the situation for the  $M_\infty \approx 1$  flows considered herein, the wake condition can be dropped. To satisfy the condition that

$$\tilde{\Phi}(x,0) = 0 \quad (-\infty < x < 0) \quad (55)$$

an additional potential,  $\Delta\tilde{\phi}$ , must be added to  $\tilde{\phi}_{\text{subsonic}}$  given by equation (40) such that  $\Delta\tilde{\phi}$  satisfies the subsonic differential equation (37), cancels the effect of  $\tilde{\phi}_{\text{subsonic}}$  ahead of the airfoil,

$$\Delta\tilde{\phi}(x,0) = -\tilde{\phi}_{\text{subsonic}}(x,0) \quad (-\infty < x < 0) \quad (56)$$

and does not alter the boundary condition satisfied by  $\tilde{\phi}_{\text{subsonic}}$  on the airfoil surface. This can be accomplished by requiring that (see ref. 1)

$$\Delta\tilde{\phi}_z(x,0) = 0 \quad (0 < x < \infty) \quad (57)$$

With these conditions, the solution for  $\Delta\tilde{\phi}$  has been found and on the x-axis is given by

$$\Delta\tilde{\phi}(x,0) = \frac{1}{\pi^2 \sqrt{-\lambda_1}} \int_0^1 f(\xi) e^{-A_1(x-\xi)} \int_0^\infty \sqrt{\frac{x}{\xi_1}} \frac{e^{-A_1(x+\xi_1)}}{x+\xi_1} \times K_0 \left[ -A_2(\xi_1 + \xi) \right] d\xi_1 d\xi \quad (58)$$

It can be shown that in the vicinity of the steady sonic point (i.e., as  $x \rightarrow x^*$ ,  $\lambda_1 \rightarrow 0$ ), the contribution of  $\Delta\tilde{\phi}$  (and its derivatives) to the unsteady pressure distribution uniformly go to zero. Consequently, the major contribution of  $\Delta\tilde{\phi}$  occurs in the vicinity of the leading edge, so that  $\Delta\tilde{\phi}$  can be regarded as essentially an edge-correction. We note that in the numerical results presented in this report,  $\Delta\tilde{\phi}$  has not been included.

#### Similarity Equations for Axisymmetric Flows

An analysis parallel to that used for the two-dimensional case has been carried out for axisymmetric flows in order to establish in that situation the governing equations and boundary conditions for the unsteady component. By splitting the potential into a steady and unsteady component,

$$\phi(x,r,t) = \phi_1(x,r) + \text{R.P.} \left\{ \tilde{\phi}(x,r) e^{i\bar{k}t} \right\} \quad (59)$$

and the normalized body ordinates in a similar fashion.

$$R(x,t) = \tau \bar{R}(x) + \text{R.P.} \left\{ \delta \tilde{R}(x) e^{i\bar{k}t} \right\} \quad (60)$$

and then using the method of matched asymptotic expansions, the potentials  $(\phi_1, \tilde{\phi})$  can be given in the following similarity form

$$\phi_1(x,r) = \varepsilon \bar{\Phi}(x,\rho) + O(\varepsilon^2) \quad (61)$$

$$\tilde{\phi}(x,r) = \varepsilon_1 \tilde{\Phi}(x,\rho) + O(\varepsilon_1^2) \quad (62)$$

where

$$\varepsilon = \tau^2 \quad (63)$$

$$\varepsilon_1 = \tau \delta \quad (64)$$

$$\rho = \tau M_\infty \sqrt{(\gamma + 1)} r \quad (65)$$

and the similarity potentials  $(\bar{\Phi}, \tilde{\Phi})$  satisfy the following differential equations and boundary conditions

$$-\left[ K_1 + \bar{\Phi}_x \right] \bar{\Phi}_{xx} + \bar{\Phi}_{\rho\rho} + \frac{1}{\rho} \bar{\Phi}_\rho = 0 \quad (66)$$

$$\lim_{\rho \rightarrow 0} (\rho \bar{\Phi}_\rho) = \bar{R}(x) \frac{d\bar{R}(x)}{dx} \quad (67)$$

$$-\left[ K_1 + \tilde{\Phi}_x \right] \tilde{\Phi}_{xx} + \tilde{\Phi}_{\rho\rho} + \frac{1}{\rho} \tilde{\Phi}_\rho = \left[ \bar{\Phi}_{xx} + iK_2 \right] \tilde{\Phi}_x - \frac{\bar{K}}{2} K_2 \tilde{\Phi} \quad (68)$$

$$\lim_{\rho \rightarrow 0} \left\{ \rho \tilde{\Phi}_\rho \right\} = \bar{R}(x) \left[ \frac{d\tilde{R}(x)}{dx} + i\bar{k}\tilde{R}(x) \right] \quad (69)$$

where  $K_1$  is given by equation (23) and

$$K_2 = \frac{2}{\gamma + 1} \frac{\bar{K}}{\varepsilon} = \frac{2}{\gamma + 1} \frac{\bar{K}}{\tau^2} \quad (70)$$

The physical pressure coefficient in this case is given by

$$C_p = \varepsilon \bar{C}_p + \varepsilon_1 \text{R.P.} \left\{ \hat{C}_p e^{i\bar{k}t} \right\} \quad (71)$$

where  $(\varepsilon, \varepsilon_1)$  are given by equations (63) and (64) and the similarity pressure coefficients  $(\bar{C}_p, \hat{C}_p)$  are defined as

$$\bar{C}_p = -2 \bar{\phi}_x - \bar{\phi}_\rho^2 \quad (72)$$

$$\hat{C}_p = -2 \left[ \tilde{\phi}_x + i k \tilde{\phi} + \bar{\phi}_\rho \tilde{\phi}_\rho \right] \quad (73)$$

Thus, the differential equation and surface boundary condition for the unsteady component  $\tilde{\phi}$  can be expressed in the form

$$\lambda_1 \tilde{\phi}_{xx} + \lambda_2 \tilde{\phi}_x + \lambda_3 \tilde{\phi} = \tilde{\phi}_{\rho\rho} + \frac{1}{\rho} \tilde{\phi}_\rho \quad (74)$$

$$\lim_{\rho \rightarrow 0} (\rho \tilde{\phi}_\rho) = g(x) \quad (75)$$

with  $\lambda_1, \lambda_2,$  and  $\lambda_3$  defined as before by equations (31), (32), and (33) and  $g(x)$  given by equation (69).

The solutions to equation (74) for constant  $(\lambda_1, \lambda_2)$  needed as the first step in the local linearization method have also been determined. They are

$$\left( \tilde{\phi}(x, \rho) \right)_{\text{sonic}} = -\frac{1}{2} \int_0^x \frac{g(\xi) \exp \left[ -\frac{\lambda_3}{\lambda_2} (x - \xi) - \frac{\lambda_2 \rho^2}{4(x - \xi)} \right]}{x - \xi} d\xi \quad (76)$$

$(\lambda_1 \approx 0)$

$$\left( \tilde{\phi}(x, \rho) \right)_{\text{super sonic}} = - \int_0^{x - \sqrt{\lambda_1} \rho} g(\xi) \times$$

$$\frac{\exp \left[ \frac{\lambda_2}{2\lambda_1} (x - \xi) \right] \cosh \left[ \frac{\lambda_2}{2\lambda_1} \sqrt{1 - \frac{4\lambda_1 \lambda_3}{\lambda_2^2}} \sqrt{(x - \xi)^2 - \lambda_1 \rho^2} \right]}{\sqrt{(x - \xi)^2 - \lambda_1 \rho^2}} d\xi \quad (77)$$

$(\lambda_1 > 0)$

$$\begin{aligned}
(\tilde{\phi}(x, \rho))_{\text{sub}} &= -\frac{1}{2} \int_0^1 g(\xi) \times \\
&\quad \frac{\exp \left[ \frac{\lambda_2}{(-2\lambda_1)} \left\{ x - \xi - \sqrt{1 - \frac{4\lambda_1\lambda_3}{\lambda_2^2}} \sqrt{(x - \xi)^2 + (-\lambda_1)\rho^2} \right\} \right]}{\sqrt{(x - \xi)^2 + (-\lambda_1)\rho^2}} d\xi \\
&\quad (\lambda_1 < 0) \tag{78}
\end{aligned}$$

#### RESULTS AND DISCUSSION

In order to illustrate the general behavior of the unsteady results predicted by the present theory, the two-dimensional unsteady local linearization equations (43), (44), and (45) have been programmed and results obtained for two types of oscillatory motions for two different classes of airfoils at  $M_\infty = 1$ . A member of the first class of airfoils (Guderley airfoils) is shown schematically in figure 1 together with its steady-state similarity pressure distribution  $\bar{C}_p$  for  $M_\infty = 1$ . These airfoils, whose normalized ordinates  $Z_1$  are given by (ref. 14),

$$Z_1(x) = \frac{25}{12} \sqrt{\frac{5}{3}} \tau(x)^{3/2} (1 - x) \tag{79}$$

are characterized by a constant steady-state surface pressure gradient  $\partial C_{p_1} / \partial x$  in the transonic Mach freeze range, i.e.,  $M_\infty \approx 1$ . Their similarity steady surface pressure distribution at  $M_\infty = 1$  is given by

$$\bar{C}_p = \frac{(\gamma + 1)^{1/3}}{\tau^{2/3}} C_{p_1} = -\frac{125}{12} \left[ \frac{9\pi}{50} \right]^{1/3} \left( x - \frac{2}{5} \right) \tag{80}$$

The second class of airfoils, shown in figure 2, is composed of parabolic-arcs with normalized ordinates given by

$$Z_1(x) = 2\tau(x - x^2) \tag{81}$$

and with similarity surface pressure distribution at  $M_\infty = 1$  represented accurately by the local linearization result (ref. 14)

$$\bar{c}_p = - 2 \left[ \frac{12}{\pi} \left( \ln [4x] - 8x + 8x^2 + \frac{3}{2} \right) \right]^{1/3} \quad (82)$$

The two types of oscillatory motions considered are vertical translation ( $\tilde{z} = 1$ ) and pitching about the nose ( $\tilde{z} = x$ ).

Figure 3 exhibits the solutions for the normalized magnitude and phase of the unsteady surface pressure distributions on the upper surface of a 6-percent thick Guderley airfoil oscillating in vertical translation (plunging) at various reduced frequencies  $\bar{k}$  at  $M_\infty = 1$ . Note that in order to provide a form more convenient for comparison, in all of the results presented herein for plunging oscillations the magnitude of the unsteady pressure distribution has been normalized by  $\delta \bar{k}$ , rather than the usual  $\delta$  since in this case  $\tilde{\phi}$  contains a linear factor in  $\bar{k}$  (see eqs. (52), (53), and (54)). The results of figure 3 illustrate the progression, for a fixed airfoil geometry as  $\bar{k}$  goes from large values to zero, of the results of the present theory as they converge smoothly to the nonlinear quasi-steady result. In particular, we note that for small values of  $\bar{k}$ , i.e.,  $\bar{k} \approx 0.1$ , the present results are close to those of quasi-steady theory, implying that in the low frequency regime, the nonlinear thickness effects of the steady flow are of primary influence on the unsteady flow and that, for very low frequencies, quasi-steady theory can provide a reasonable approximation.

While figure 3 demonstrates the ability of the present theory to converge uniformly to the nonlinear quasi-steady result as  $\bar{k} \rightarrow 0$ , figure 4 shows the corresponding ability, as  $\bar{k}$  becomes large, of the present theory to converge to linear acoustic theory results. For low  $\bar{k}$  (i.e.,  $\bar{k} = 0.1$ ), figure 4 clearly indicates that linear theory is virtually useless (the phase angle for  $\bar{k} = 0.1$  is off the scale of the plot), while at larger values ( $\bar{k} = 2$ ), the results of the present nonlinear theory and linear acoustic theory are converging. At  $\bar{k} = 5$ , the results are essentially identical.

Figures 5 and 6 show the analogous results of figures 3 and 4 for a 6-percent thick parabolic-arc airfoil. Figure 5 demonstrates that, as was the case for the Guderley airfoil, the present theory moves smoothly

toward the quasi-steady result as  $\bar{k}$  becomes small, while figure 6 illustrates the corresponding convergence to linear theory as  $\bar{k}$  becomes large. In particular, we note in comparing figures 4 and 6, that as  $\bar{k}$  becomes large, the results for both the Guderley airfoil and the parabolic-arc airfoil uniformly approach each other (as well as linear theory), which agrees with the concept that for large  $\bar{k}$  the unsteady motion becomes independent of the profile geometry.

In figure 7(a) and (b), the normalized magnitude ( $|\tilde{C}_p|/\delta$ ) and phase of the unsteady pressure distribution are presented for a 6-percent thick Guderley airfoil oscillating in pitch about the nose at  $M_\infty = 1$ . For this unsteady motion, we note again the smooth variation of the present theory to the quasi-steady result as  $\bar{k} \rightarrow 0$ . Figure 8(a) and (b) compares these same results with linear theory. This figure demonstrates that for pitching oscillations, as was the case for plunging motion, linear theory is in serious error for  $\bar{k}$  less than 1. For  $\bar{k} = 2$ , the magnitude of  $\tilde{C}_p$  predicted by linear theory is in good agreement with the present nonlinear results while the phase is only in fair agreement. At  $\bar{k} = 5$ , both magnitude and phase are essentially identical to the present theory. Figures 9(a) and (b) and 10(a) and (b) show the corresponding results for a 6-percent thick parabolic-arc airfoil. These demonstrate virtually the same behavior as those shown for the Guderley airfoil.

Since all the results presented thus far have been for a fixed thickness ratio, in order to demonstrate explicitly the importance of nonlinear thickness effects we have prepared figure 11 which shows, for a fixed reduced frequency ( $\bar{k} = 0.1$ ), the normalized magnitude ( $|\tilde{C}_p|/\delta\bar{k}$ ) and phase of the unsteady surface pressure due to plunging oscillations of various thickness-ratio parabolic-arc airfoils. We note the enormous change in both magnitude and phase as  $\tau$  increases only slightly from zero (for which the present theory and linear acoustic theory are the same) to one-percent thickness ratio ( $\tau = 0.01$ ). These results demonstrate quantitatively both the importance of thickness effects and the inadequacy of linear theory at low frequencies, even for exceptionally thin airfoils. Figure 12 shows similar results for the higher reduced frequency  $\bar{k} = 1.0$ . In this case, the differences in the magnitude of the unsteady pressures for the various thickness ratios are not nearly as great as for  $\bar{k} = 0.1$  and also are largely restricted to the aft portion of the airfoil. The

phase angles, which are generally more sensitive to change remain somewhat separated for each thickness ratio. Nevertheless, the trend of all the curves to move toward the zero thickness (linear) result is clear. This trend is notably demonstrated in figure 13 which shows the analogous results for  $\bar{k} = 10$ . In this case, there is essentially no difference in the magnitude or phase angle for the various thickness ratios from the linear ( $\tau = 0.0$ ) result, except near the tail, where presumably the flow finally has had enough time to react to some of the nonlinear effects of thickness in the steady flow.

#### CONCLUDING REMARKS

Theoretical analysis has been carried out to develop the basis of a nonlinear, unsteady, small-disturbance theory valid for all frequencies which is capable of predicting transonic inviscid flows about thin airfoils undergoing both rigid body and elastic oscillations at  $M_\infty \approx 1$ . The theory employs the concept of dividing the flow into steady and unsteady components and then solves, by the method of local linearization, the coupled unsteady equation for the surface pressure distribution.

Calculated results for two classes of airfoils and two types of oscillatory motions indicate smooth convergence to the quasi-steady results as the reduced frequency based on chord  $\bar{k} \rightarrow 0$  and to linear acoustic results as  $\bar{k}$  becomes large ( $\bar{k} \geq 2$ ). Moreover, at low frequencies ( $\bar{k} \approx 0.1$ ) the theory demonstrates quantitatively both the large nonlinear thickness effects induced on the unsteady flow by the steady motion and the subsequent inadequacy of linear theory in this frequency regime.

Application to more complex aerodynamic configurations is possible, as shown by the derivation and partial solution of the corresponding results for unsteady axisymmetric flows. At this stage of development, several details of the theory remain to be worked out. For example, the proper unsteady shock relations need to be determined and applied, both to surface and bow shocks, and several questions concerning the error incurred in the unsteady surface pressure by using the local linearization approximation need to be investigated. Experimental verification of the theory is essential at this stage and while we are unaware of any data suitable for comparison with the preliminary results presented herein,

future work should be directed toward those configurations for which experimental data exists. Finally, the results obtained in this preliminary investigation strongly suggest that further development and analysis, to extend and refine this promising technique, be carried out as soon as possible in order to provide a practical and accurate aerodynamic tool for analyzing unsteady transonic flutter and stability problems.

Nielsen Engineering & Research, Inc.  
Mountain View, California  
November, 1972

## REFERENCES

1. Landahl, M. T.: Unsteady Transonic Flow. Pergamon Press, London, 1961.
2. Oswatitsch, K.: Quellen in schallnaher Strömung. In Symposium Transsonicum, K. Oswatitsch, ed., Springer-Verlag, Berlin/Göttingen/Heidelberg, 1964, pp. 402-413.
3. Landahl, M. T.: Linearized Theory for Unsteady Transonic Flow. In Symposium Transsonicum K. Oswatitsch, ed., Springer-Verlag, Berlin/Göttingen/Heidelberg, 1964, pp. 414-439.
4. Stark, V. J.: Applications at  $M = 1$  of a Method for Solving the Subsonic Problem of the Oscillating Finite Wing with the Aid of High-Speed Digital Computers. In Symposium Transsonicum, K. Oswatitsch, ed., Springer-Verlag, Berlin/Göttingen/Heidelberg, 1964, pp. 440-455.
5. Garabedian, P. R. and Korn, D. G.: Numerical Design of Transonic Airfoils. Numerical Solution of Partial Differential Equations - II, Bert Hubbard, ed., Academic Press, Inc., 1971, pp. 253-271.
6. Murman, E. M. and Cole, J. D.: Calculation of Plane Steady Transonic Flows. AIAA Jour., Vol. 9, No. 1, Jan. 1971, pp. 114-121.
7. Murman, E. M. and Krupp, J. A.: The Numerical Calculation of Steady Transonic Flows Past Thin Lifting Airfoils and Slender Bodies. AIAA Paper No. 71-566, presented at AIAA 4th Fluid and Plasma Dynamics Conference, Palo Alto, CA, June 21-23, 1971.
8. Spreiter, J. R. and Stahara, S. S.: Calculative Techniques for Transonic Flows About Certain Classes of Airfoils and Slender Bodies, NASA CR-1722, 1971.
9. Stahara, S. S. and Spreiter, J. R.: Calculative Techniques for Transonic Flows About Certain Classes of Slender Wing-Body Combinations. NASA CR-2103, 1972.
10. Stahara, S. S. and Spreiter, J. R.: Calculative Techniques for Transonic Flows About Certain Classes of Slender Wing-Body Combinations - Phase II. NASA CR-2157, 1972.
11. Guderley, K. G.: Theory of Transonic Flow. Pergamon Press, Oxford, England, 1962.
12. Ferrari, C. and Tricomi, F.: Transonic Aerodynamics. Academic Press, New York, 1968.
13. Miles, J. W.: The Potential Theory of Unsteady Supersonic Flow. Cambridge University Press, 1959.

14. Spreiter, J. R. and Alksne, A. Y.: Thin Airfoil Theory Based on Approximate Solution of the Transonic Flow Equation. NACA TR 1359, 1958. (Supersedes NACA TN 3970.)
15. Spreiter, J. R.: Aerodynamics of Wings and Bodies at Transonic Speeds. Jour. Aero/Space Sci., Vol. 26, No. 8, Aug. 1959, pp. 465-487.
16. Spreiter, J. R.: The Local Linearization Method in Transonic Flow Theory. In Symposium Transsonicum, K. Oswatitsch, ed., Springer-Verlag, Berlin/Göttingen/Heidelberg, 1964, pp. 92-109.
17. Alksne, A. Y. and Spreiter, J. R.: Theoretical Pressure Distribution on Wings of Finite Span at Zero Incidence for Mach Numbers Near 1. NASA Rep. R-88, 1961.
18. Spreiter, J. R. and Alksne, A. Y.: Slender Body Theory Based on Approximate Solution of the Transonic Flow Equation. NASA TR R-2, 1959.
19. Spreiter, J. R., Smith, D. W., and Hyett, B. J.: A Study of the Simulation of Flow with Free-Stream Mach Number 1 in a Choked Wind Tunnel. NASA TR R-73, 1960.

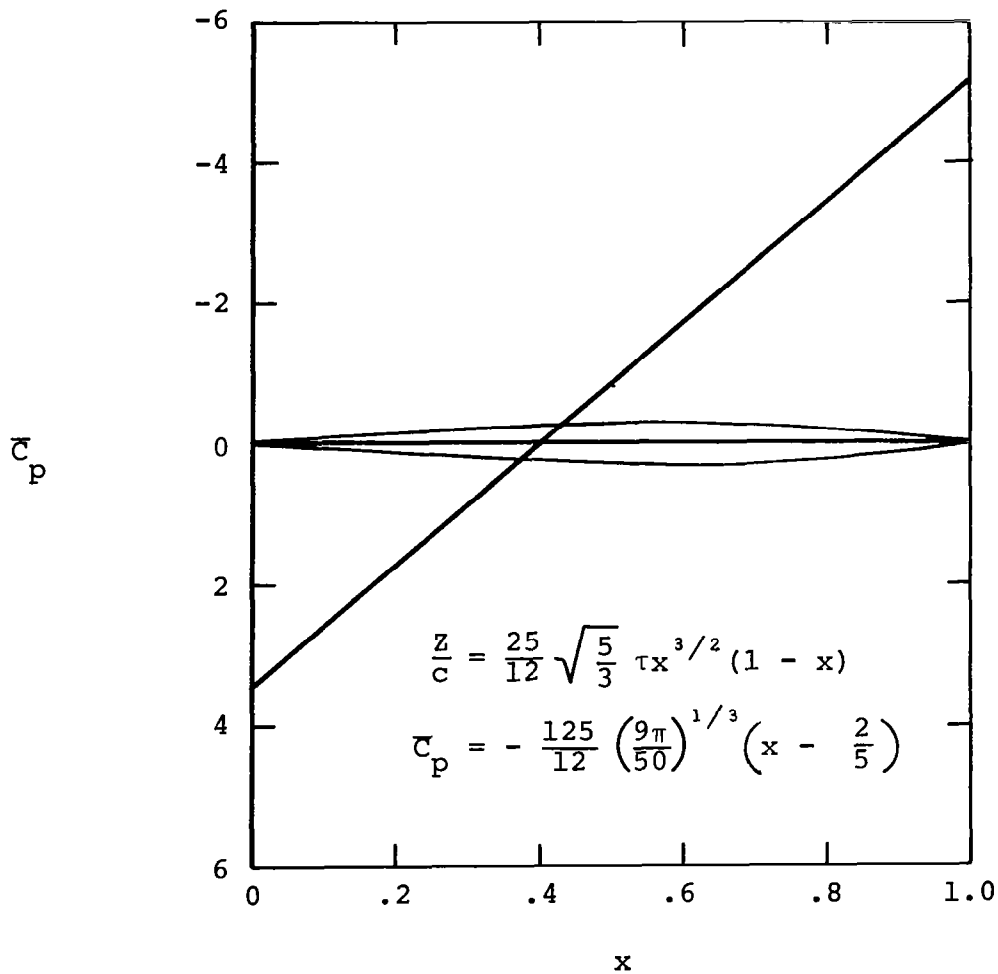


Figure 1.-Similarity form of steady surface pressure distribution for a family of affinely-related Guderley airfoils at  $M_\infty = 1$  according to the method of local linearization.

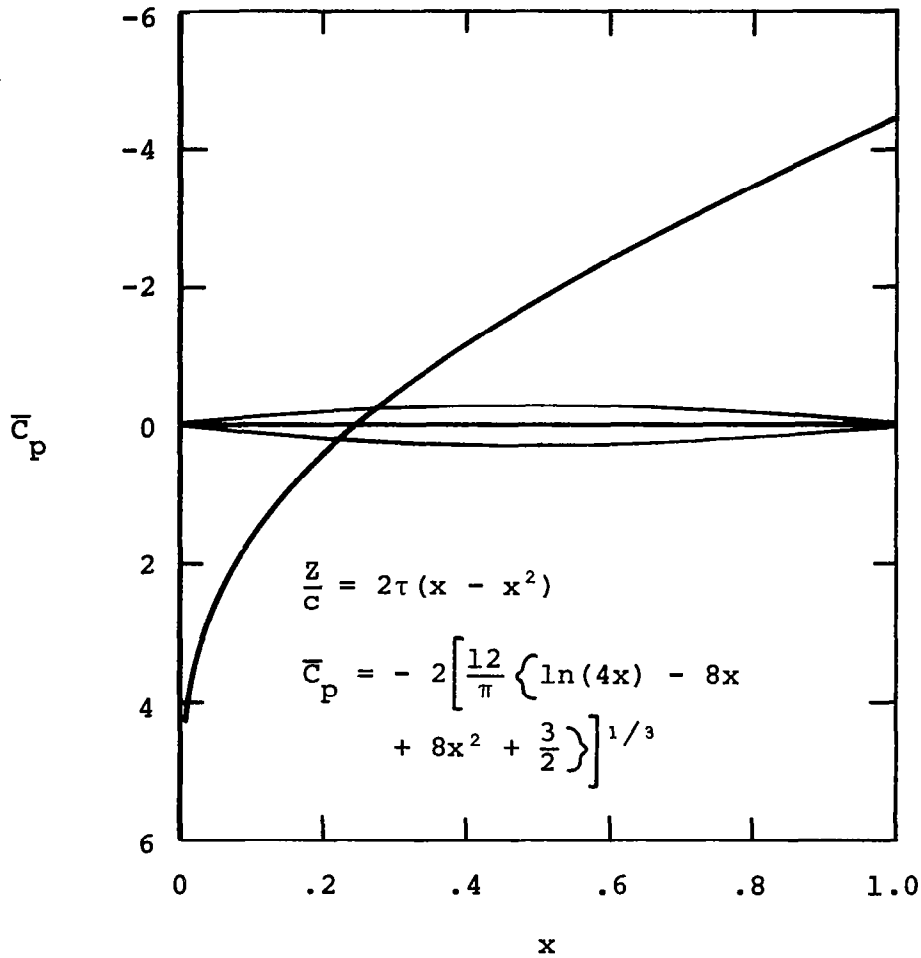


Figure 2.-Similarity form of steady surface pressure distribution for a family of affinely-related parabolic-arc airfoils at  $M_\infty = 1$  according to the method of local linearization.

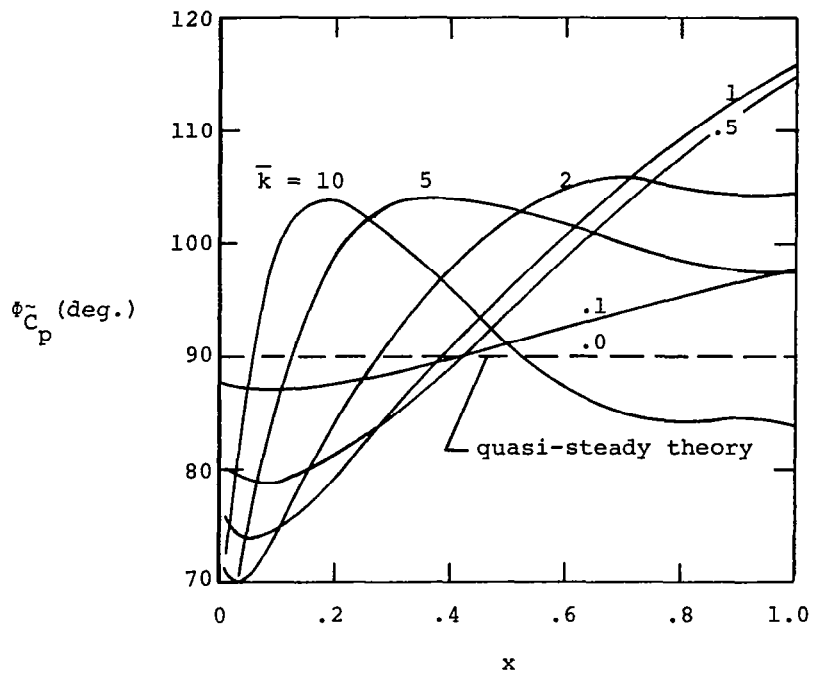
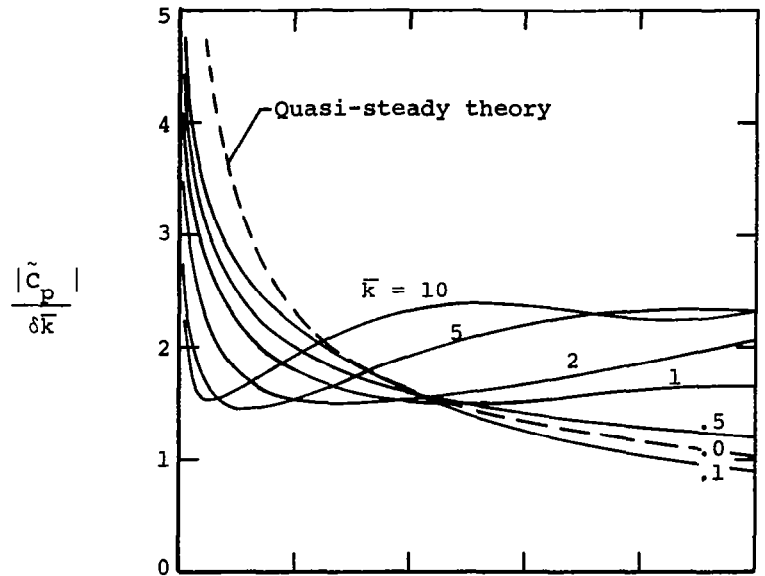


Figure 3.-Magnitude and phase of unsteady pressure distributions on the upper surface of a 6-percent thick Guderley airfoil oscillating in vertical translation at various reduced frequencies  $\bar{k}$  at  $M_\infty = 1$ .

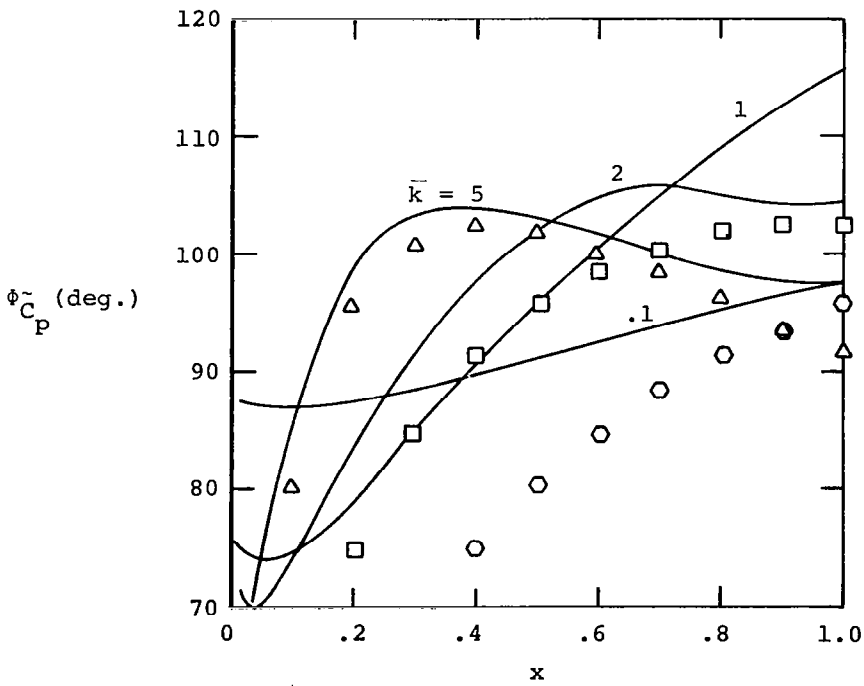
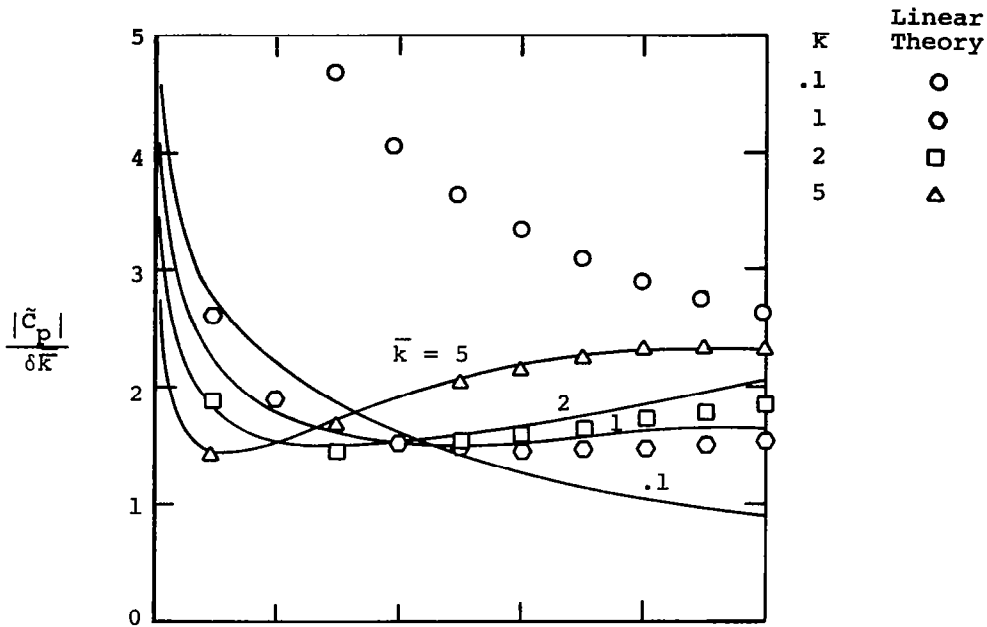


Figure 4.-Comparisons of local linearization unsteady pressure distributions given in Figure 3 with linear theory.

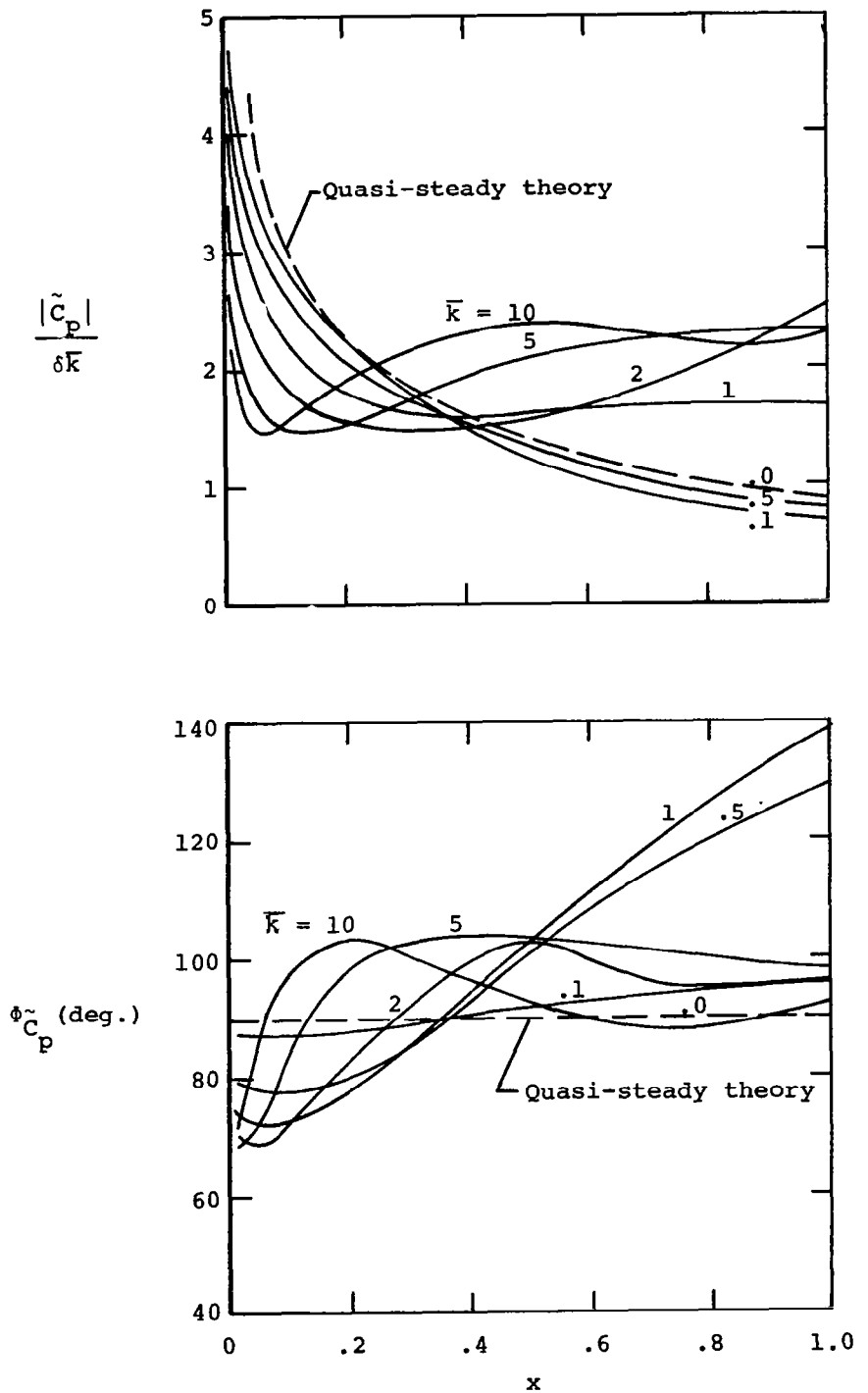


Figure 5.-Magnitude and phase of unsteady pressure distributions on the upper surface of a 6-percent thick parabolic-arc airfoil oscillating in vertical translation at various reduced frequencies  $\bar{k}$  at  $M_\infty = 1$ .

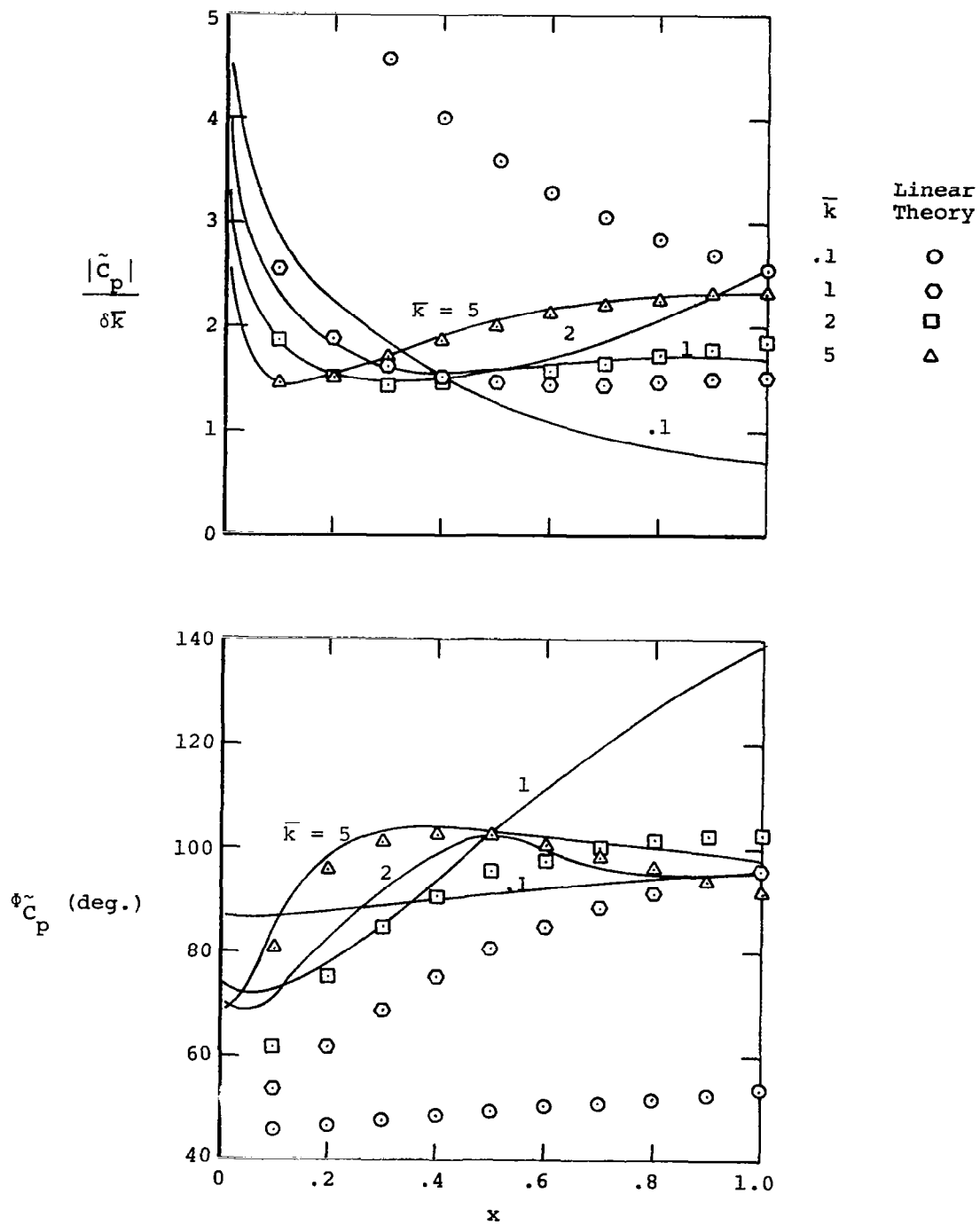


Figure 6.-Comparisons of local linearization unsteady pressure distributions given in Figure 5 with linear theory.

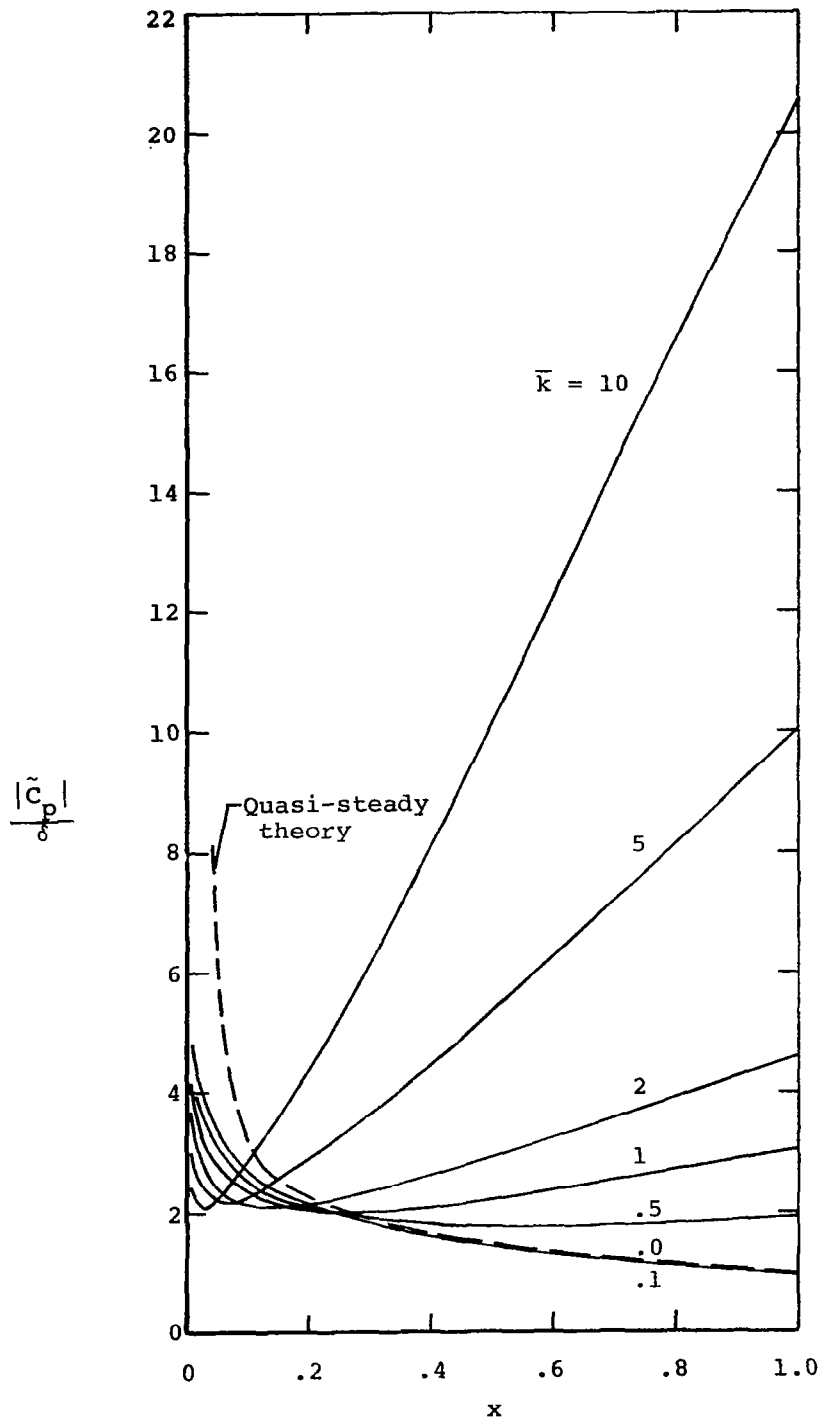


Figure 7(a).-Magnitude of unsteady pressure distributions on the upper surface of a 6-percent thick Guderley airfoil oscillating in pitch about the nose at various reduced frequencies  $\bar{k}$  at  $M_\infty = 1$ .

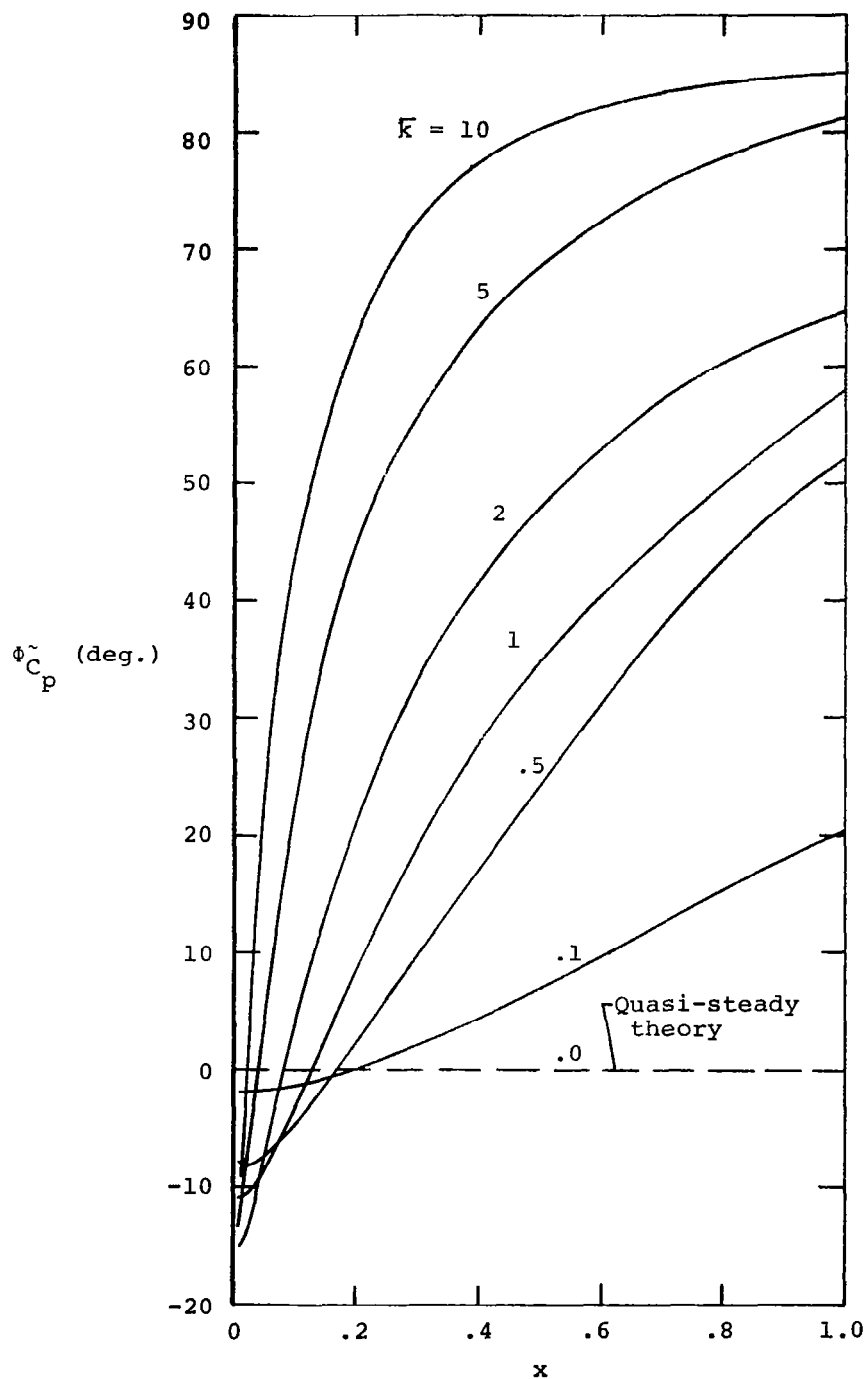


Figure 7(b).-Phase of unsteady pressure distributions on the upper surface of a 6-percent thick Guderley airfoil oscillating in pitch about the nose at various reduced frequencies  $\bar{K}$  at  $M_\infty = 1$ .

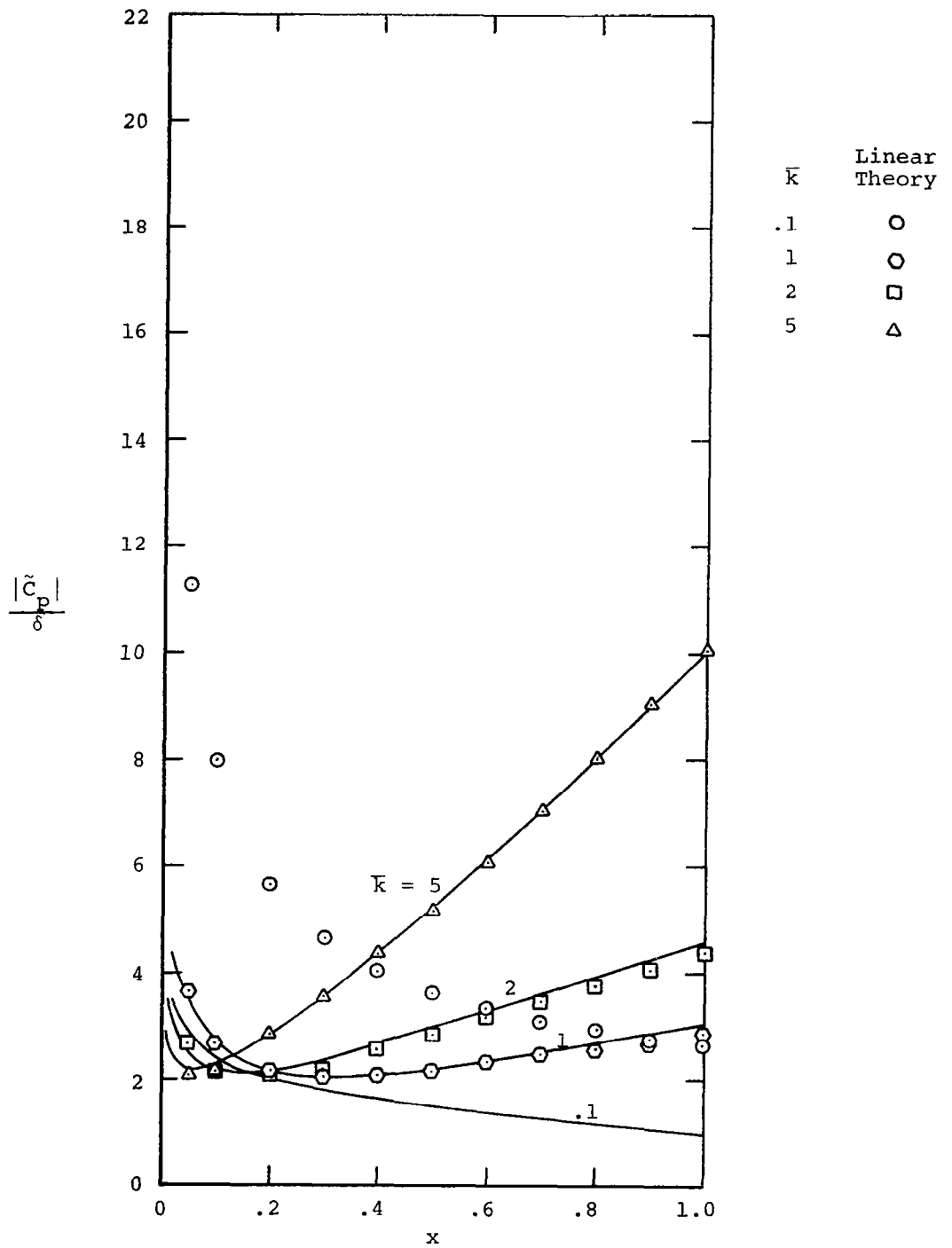


Figure 8(a).-Comparisons of the magnitude of the local linearization unsteady pressure distributions given in Figure 7(a) with linear theory.

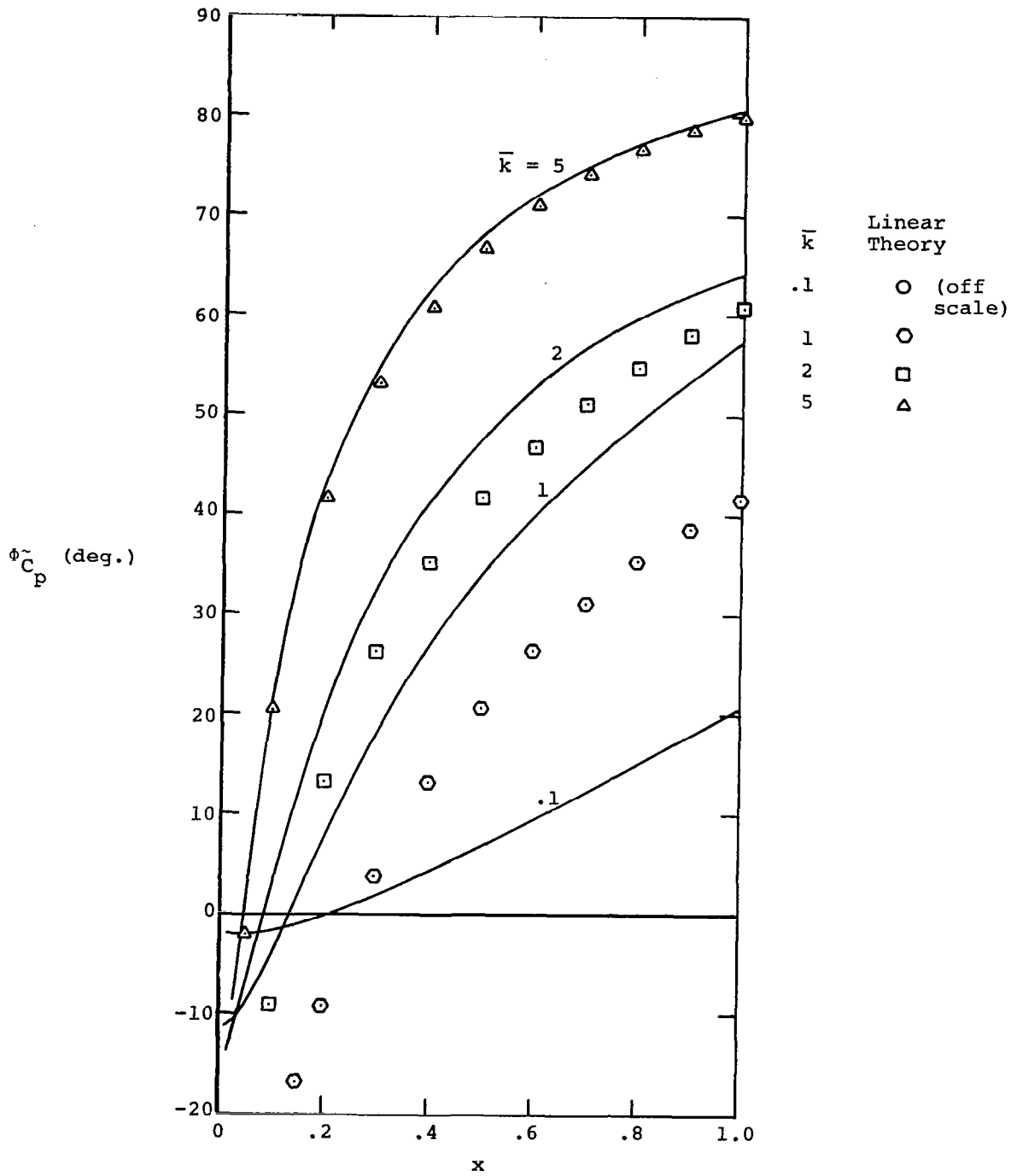


Figure 8(b).--Comparisons of the phase of the local linearization unsteady pressure distributions given in Figure 7(b) with linear theory.

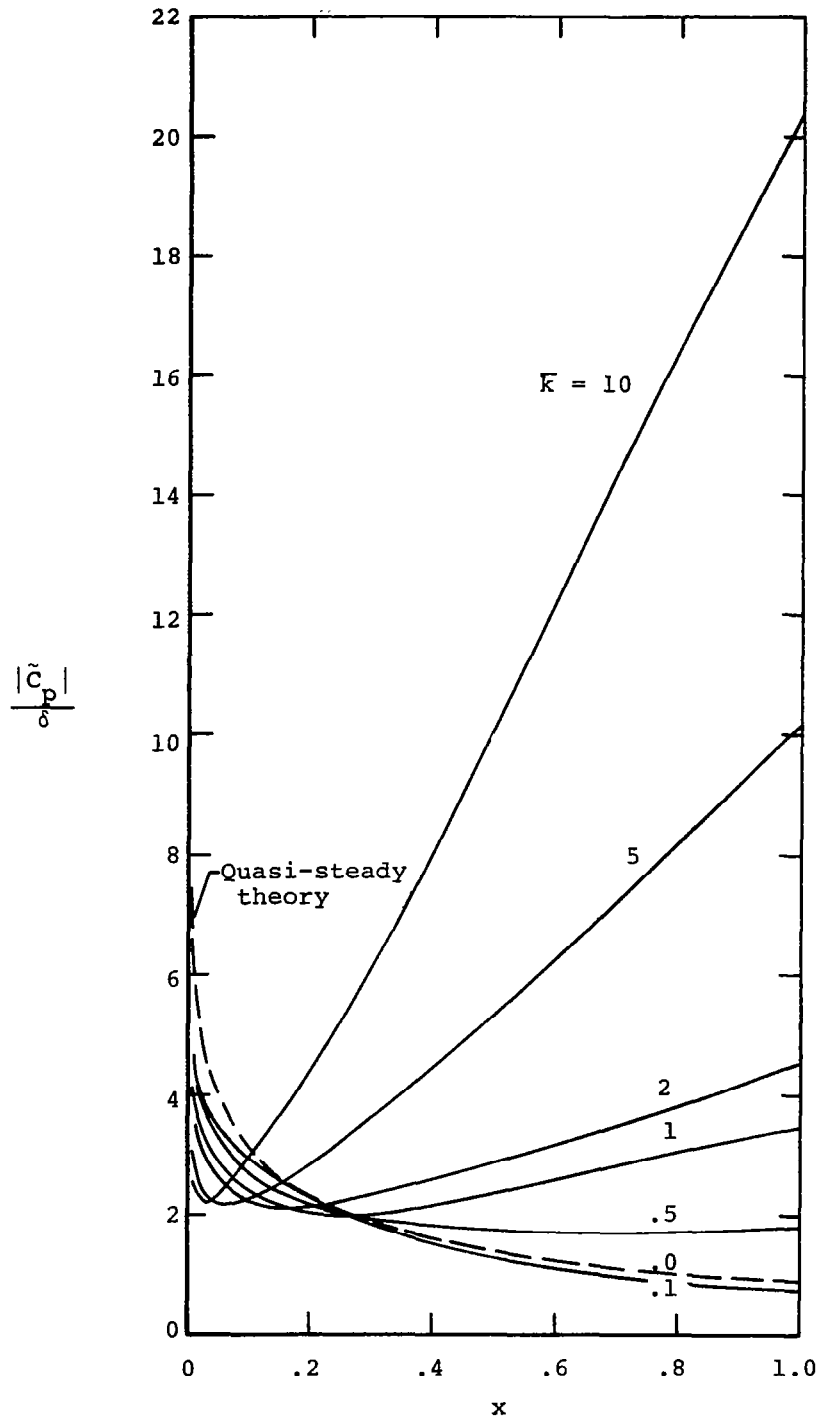


Figure 9(a).—Magnitude of unsteady pressure distributions on the upper surface of a 6-percent thick parabolic-arc airfoil oscillating in pitch about the nose at various reduced frequencies  $\bar{K}$  at  $M_\infty = 1$ .

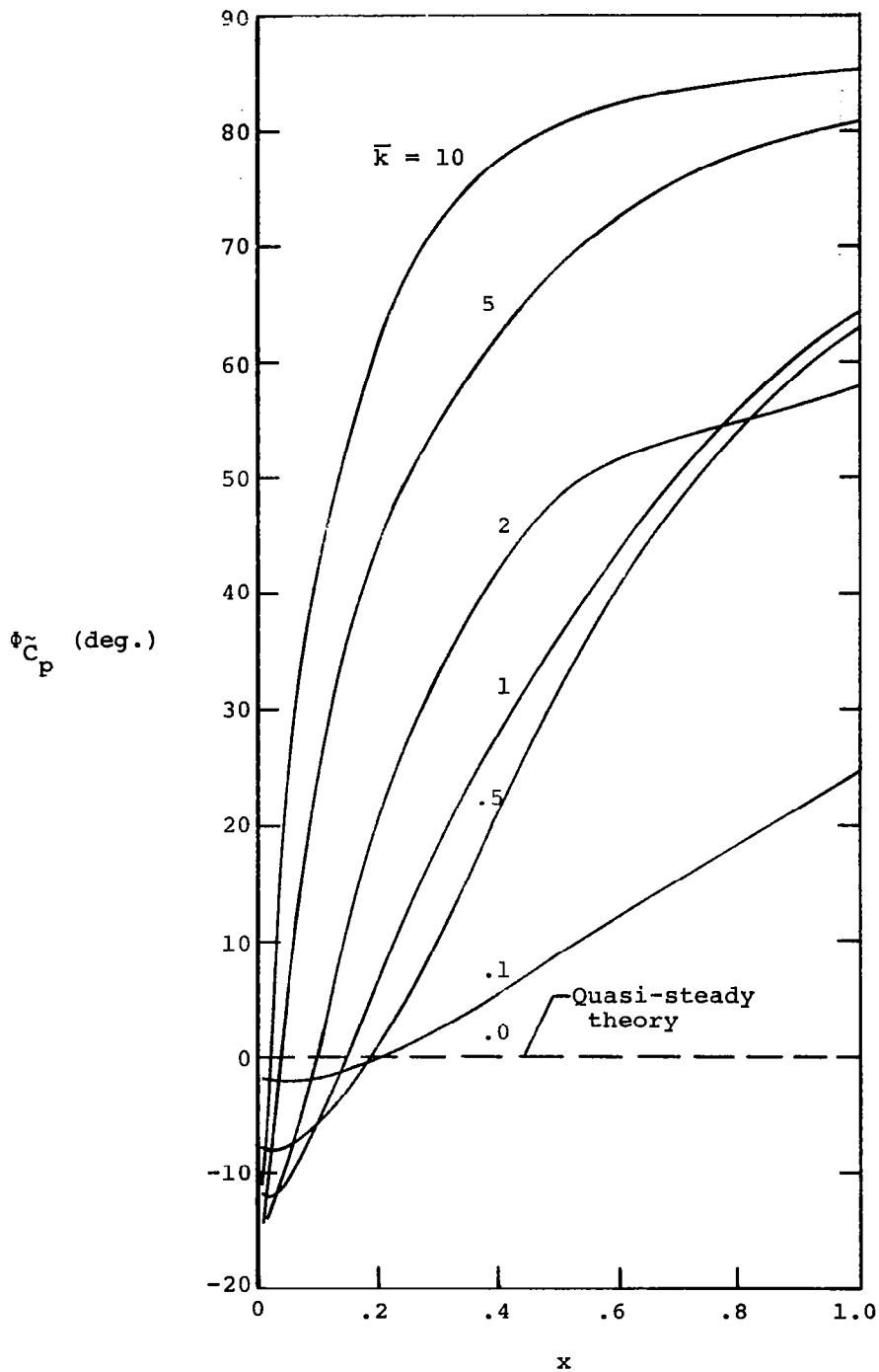


Figure 9(b).—Phase of unsteady pressure distributions on the upper surface of a 6-percent thick parabolic-arc airfoil oscillating in pitch about the nose at various reduced frequencies  $\bar{k}$  at  $M_\infty = 1$ .

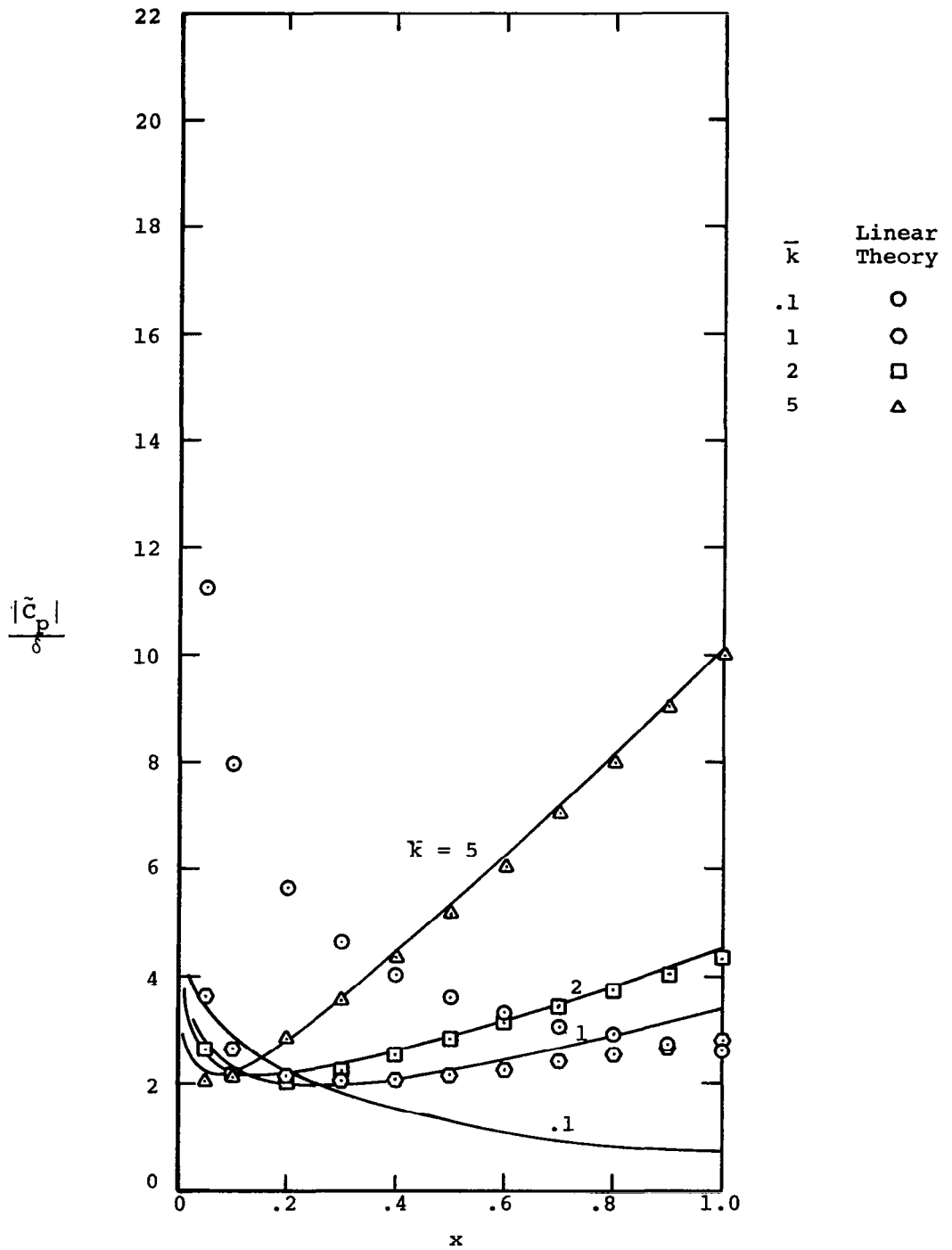


Figure 10(a).—Comparisons of the magnitude of the local linearization unsteady pressure distributions given in Figure 9(a) with linear theory.

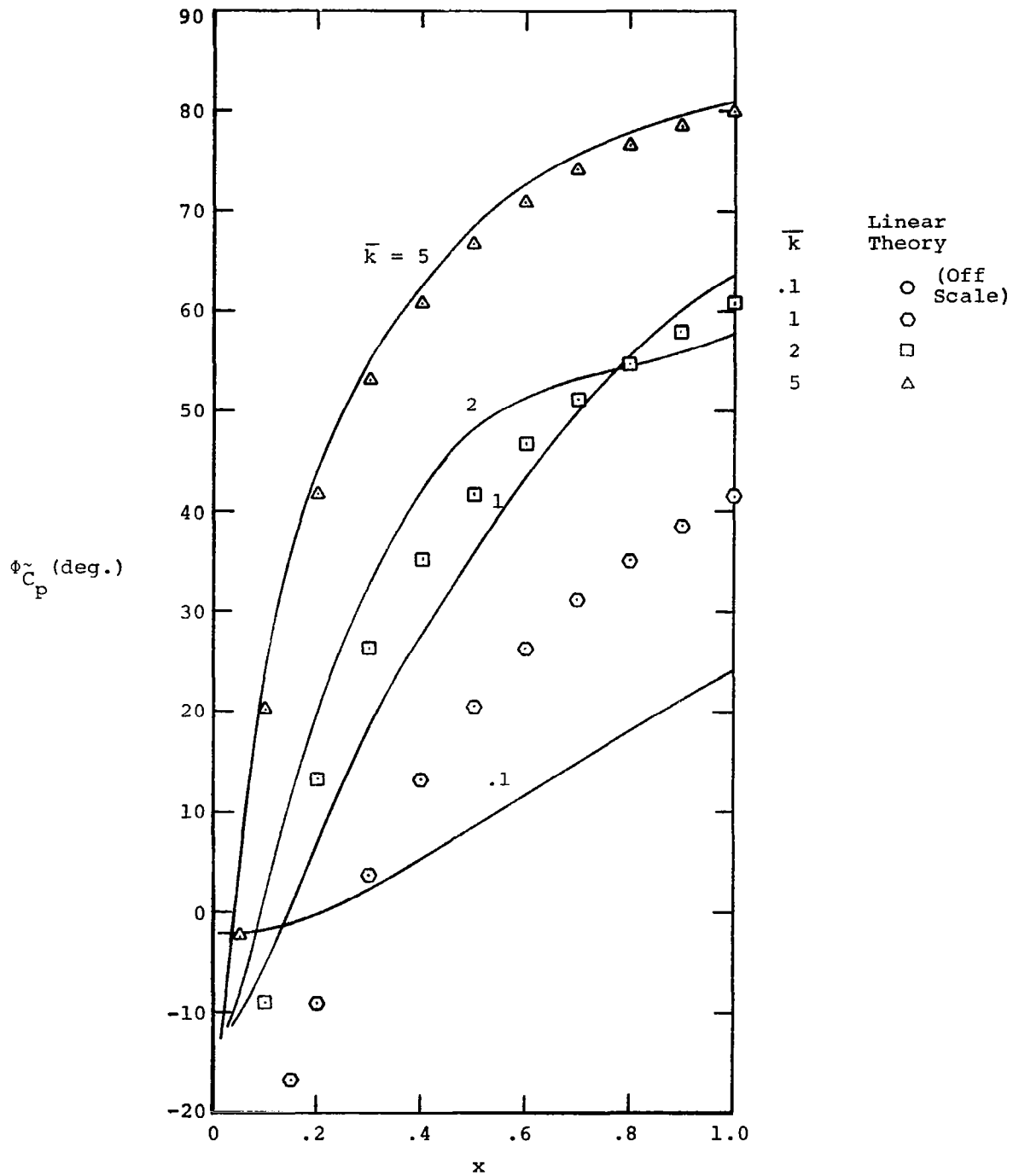


Figure 10(b).-Comparisons of the phase of the local linearization unsteady pressure distributions given in Figure 9(b) with linear theory.

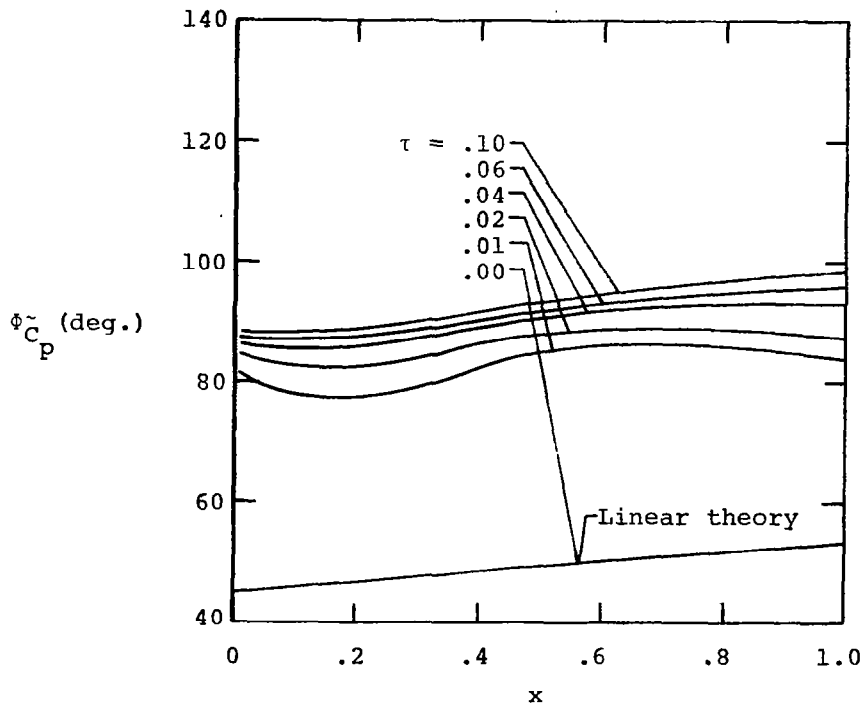
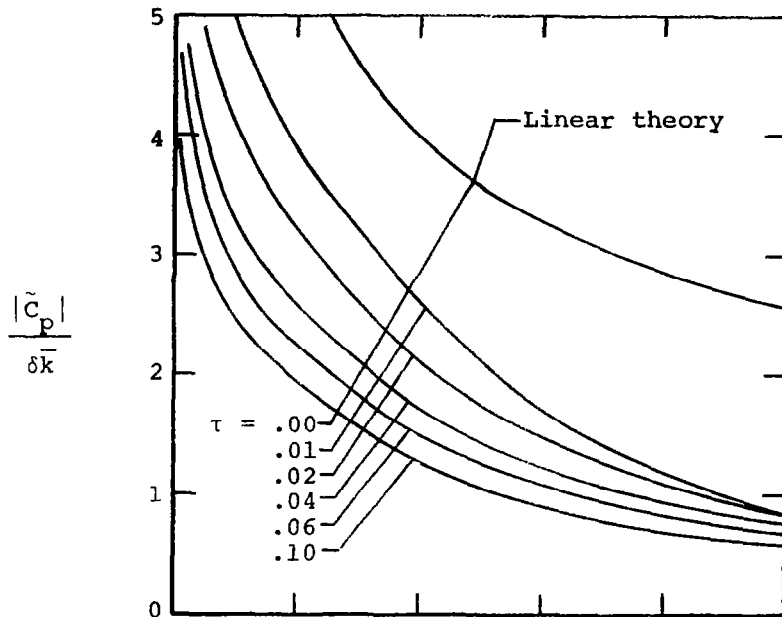


Figure 11.-Magnitude and phase of unsteady pressure distributions on the upper surface of parabolic-arc airfoils having various thickness ratios oscillating in vertical translation at the reduced frequency  $K = 0.1$  with  $M_\infty = 1$ .

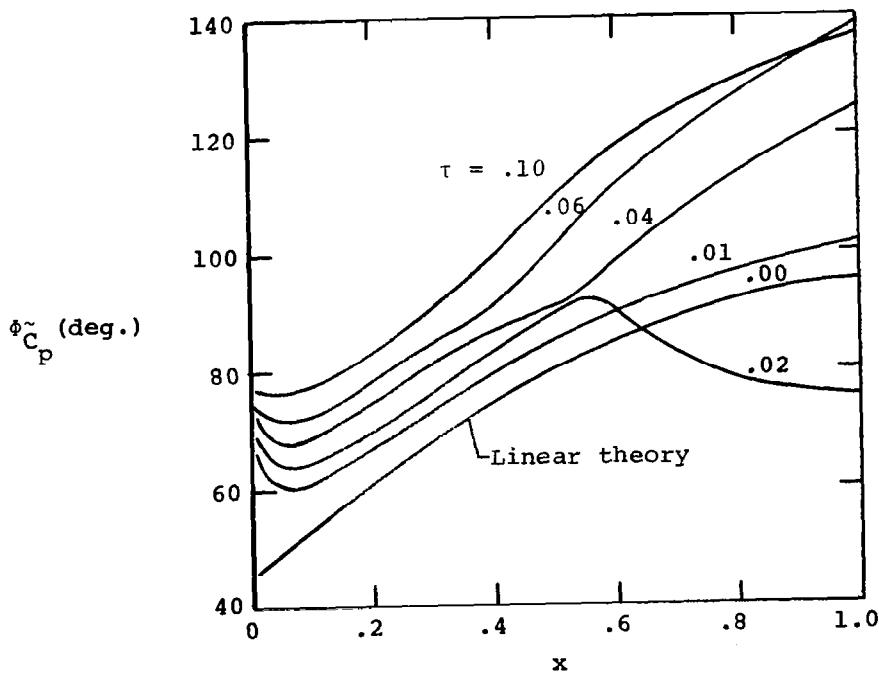
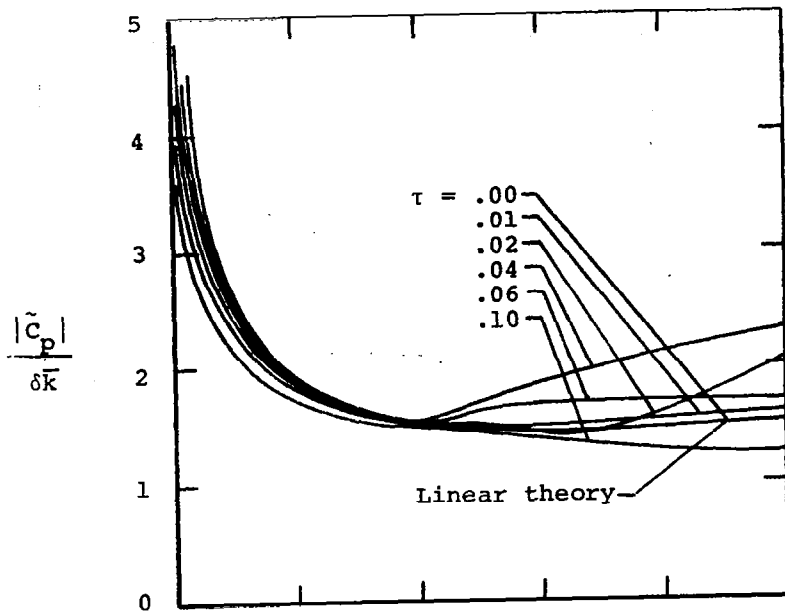


Figure 12.--Magnitude and phase of unsteady pressure distributions on the upper surface of parabolic-arc airfoils having various thickness ratios oscillating in vertical translation at the reduced frequency  $\bar{K} = 1.0$  with  $M_\infty = 1$ .

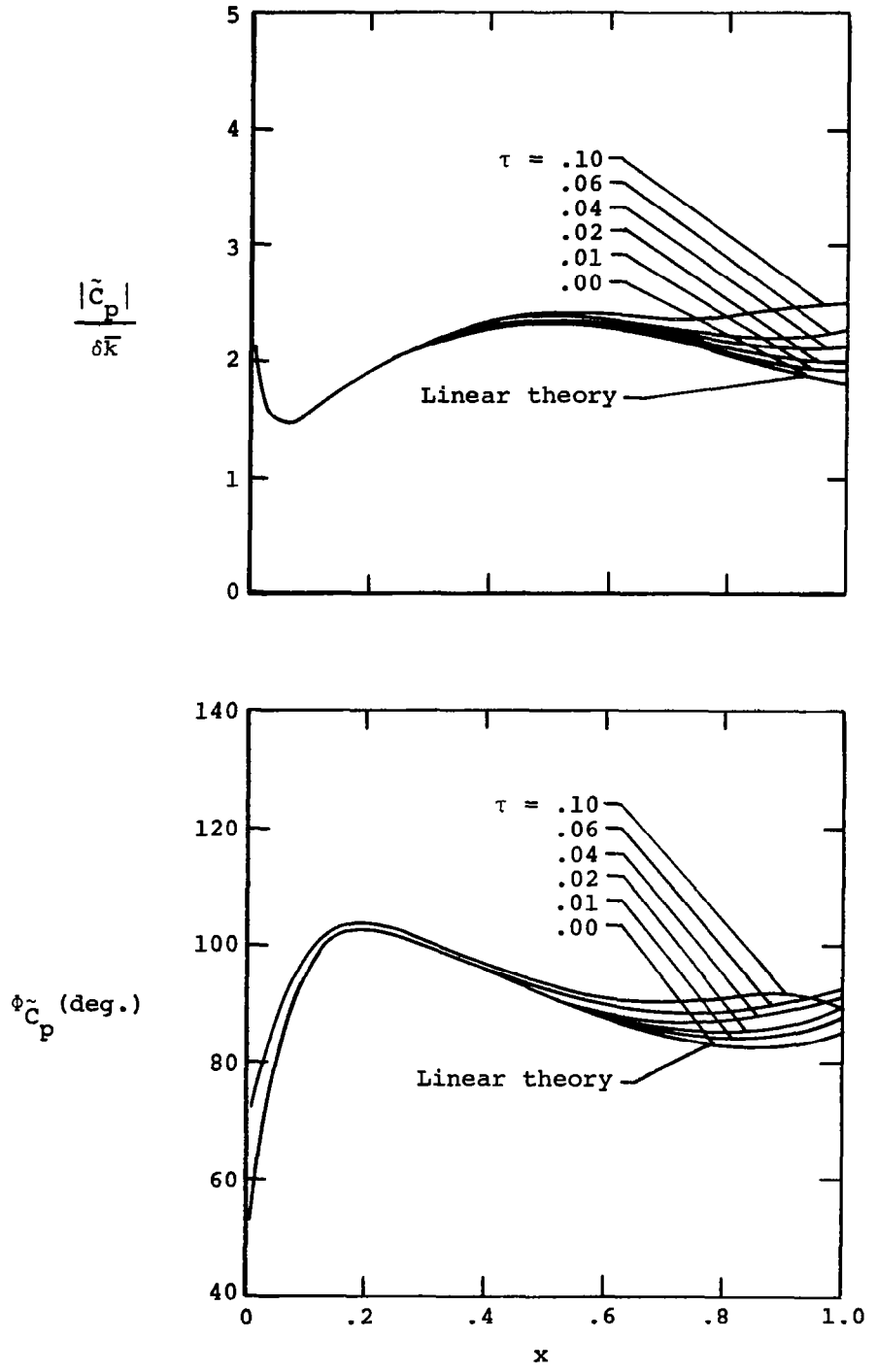


Figure 13.-Magnitude and phase of unsteady pressure distributions on the upper surface of parabolic-arc airfoils having various thickness ratios oscillating in vertical translation at the reduced frequency  $\bar{k} = 10$ . with  $M_\infty = 1$ .